DESIGN, CONSTRUCTION, AND CONTROL OF AN AUTONOMOUS HUMANOID ROBOT

BY

SCOTT D. NORTMAN

A THESIS PRESENTED TO THE GRADUATE SCHOOL
OF THE UNIVERSITY OF FLORIDA IN PARTIAL FULFILLMENT
OF THE REQUIREMENTS FOR THE DEGREE OF
MASTER OF SCIENCE

UNIVERSITY OF FLORIDA

2002

ACKNOWLEDGMENTS

I would like to thank my family for all of their love and support and my soon to be in-laws for the extra motivation. I also want to thank Dr. Arroyo for being supportive, always making me laugh in class, and allowing me to pursue my ideas, Dr. Schwartz for influencing me to pursue *Pneuman* and for entertaining ideas about what *Pneuman* will look like when finished, and Dr. Nechyba for the overwhelming number of questions, answers, and the explanations of how things work. Finally, I would like to thank the most important person in my life, Meredith. Without my beautiful fiancee, this thesis would not exist. I thank her for all of the love, support, kindness, and inspiration she has given to me.

TABLE OF CONTENTS

page

ACKNOWLEDGMENTS ii

ABSTRACT vii

CHAPTER

1 INTRODUCTION 1

- 1.1 Historical Perspective 1
- 1.2 Literature Review 4
- 1.3 This Work 10

2 PHYSICAL STRUCTURE 13

- 2.1 Overall Design Considerations 13
- 2.2 Specifications 15
- 2.3 Drive System. 18
- 2.4 Kinematics 23

3 ELECTRONIC SYSTEMS 31

- 3.1 Overview. 31
- 3.2 Power System 32
- 3.3 Computer System 32
- 3.4 Pulse Width Modulation (PWM) System 34
- 3.5 Hardware-Implemented Control System 35
- 3.6 Solid State Motor Drivers 37

4 CONTROL THEORY 39

- 4.1 Overview. 39
- 4.2 Control of Direct Current (DC) Motors 39
- 4.3 Control System Implementation 41
- 4.4 Joint Trajectory Generation 46

5 USER INTERFACE 53

6 DISCUSSION, FUTURE WORK, AND CONCLUSION 57

  6.1 Discussion 57
  6.2 Future Work 58
  6.3 Conclusion 60

APPENDIX

A MECHANICAL DRAWINGS 62

B SCHEMATICS 63

REFERENCES 65

BIOGRAPHICAL SKETCH 68

LIST OF FIGURES

figure page

1-1 The Cittern Player. 2

1-2 Honda’s humanoid robot, the P3. 5

1-3 NASA’s humanoid robot, Robonaut.. 6

1-4 Electrotechnical Laboratory’s robot, the ETL-humanoid.. 7

1-5 Pneumatically actuated humanoid robot.. 8

1-6 MIL’s first humanoid, Omnibot 2000.. 10

1-7 University of Florida’s humanoid, Pneuman. 12

2-1 Pneuman’s overall dimensions. 16

2-2 Pneuman’s original design. 16

2-3 The instantaneous center of curvature, I.C.C. 19

2-4 Skid steering. 20

2-5 Ackerman steering. 21

2-6 Four-wheel or “crab” steering.. 21

2-7 The base and wheel assemblies. 22

2-8 Pneuman’s active stereo head. 23

2-9 Epipolar plane formed by two cameras and the object. 24

2-10 One of Pneuman’s robotic arms. 25

2-11 Kinematic representation of Pneuman’s arms. 25

2-12 Coordinate frame assignment for arms. 26

2-13 Kinematic figure of Pneuman’s waist joint. 29

2-14 Pneuman’s waist joint.. 30

3-1 Block diagram of Pneuman’s electronics and control systems.. 31

3-2 Pneuman’s battery and power system.. 32

3-3 Software structure. 33

3-4 Pulse width modulation system. 35
3-5 Analog to digital conversion system.. 36
3-6 Image of the PWM and A to D pc/104 card. 36
3-7 Image of LM629 pc/104 card. 37
3-8 Block diagram of the H-bridge motor driver. 38
3-9 Solid state H-bridge motor driver. 38
4-1 Pulse width modulation 41
4-2 Block diagram of analog control system. 42
4-3 Output of uncalibrated potentiometer 43
4-4 Calibrated potentiometer plot 44
4-5 LM629 PID controller block diagram. 45
4-6 Plot of desired cubic trajectory 50
4-7 Trajectory with via points. 51
4-8 Typical LM629 Motion Trajectories 52
5-1 Initial Startup Screen of User Interface 53
5-2 Parameters menu.. 54
5-3 Setting the desired position of the left front steering joint. 54
5-4 Real-time plot of desired, actual, and error trajectory values. 55
5-5 Calibration Utility 56
5-6 Drive Control Menu. 56
6-1 Augmented control scheme 59
A-1 Pneuman’s overall dimentions. 62
B-1 PWM pc/104 card schematic 63
B-2 LM629 pc/104 card schematic. 64

Abstract of Thesis Presented to the Graduate School
of the University of Florida in Partial Fulfillment of the
Requirements for the Degree of Master of Science

DESIGN, CONSTRUCTION, AND CONTROL OF AN AUTONOMOUS HUMANOID ROBOT

By

Scott D. Nortman

May, 2002

Chairman: Dr. A. Antonio Arroyo
Major Department: Electrical and Computer Engineering

From the beginning of time, humans have attempted to recreate themselves, first as drawings on cave walls, then as statues, and finally as humanoid robots. Humanoid robots have been popularized by science fiction for decades through books and movies. Fortunately, with today's rapidly advancing technology, science fact is getting closer to science fiction. Humanoid robot research and development are global phenomena, with new projects emerging everyday. This paper details one of these humanoid projects. Information regarding the current state of the art is presented and discussed, and *Pneuman,* a humanoid robot, is discussed in detail. Design considerations, construction details, and control issues are presented and explained.

CHAPTER 1
INTRODUCTION

1.1 Historical Perspective

“The ultimate quest, the Grail of many roboticists today, is to build a humanoid robot,” stated Peter Menzel and Faith D’Alusio, after visiting the world's top robotics research labs to learn about the current state-of-the-art humanoids for their book *Robosapiens: Evolution of a New Species* [1:18]. But why do robotics researchers feel this way? The answer can by found in history.

The human form was idealized from the beginning of recorded time. The first known civilizations in Egypt had many skilled craftsmen that made human or human-like figures. Most were used for religious purposes, others for decoration. The familiar sculptures of Queen Nefertiti, the Tutankhamen sarcophagus, and the Sphinx all came from this civilization [2]. Additionally, Egyptian hieroglyphics contain pictures and references to human and human-like figures [3]. Another well know ancient civilization existed in ancient Greece. Greek artists are responsible for a countless numbers of human sculptures, including the great bronze Zeus, The Chryselephantine Snake Goddess, Hercules, Venus de Milo, and many more [4].

While these early attempts to recreate the human form illustrate the skills of the sculptors, they still lacked an obvious human attribute; *movement*. The mechanisms needed to animate statues had not yet been invented. Over time, however, the Greeks began to apply their knowledge of pneumatic and hydraulic systems, providing movement for small figurines and statues [5]. The first moving statues were made by the Greek engineer Ctesibius in approximately 200 B.C.E. His work, along with other Greek engineers, include numerous moving scenes, such as Hercules shooting a snake, Hercules slaying a dragon, and singing birds at a fountain [6].

Perhaps the best know pre-modern engineer is Leonardo da Vinci. He studied many of the Greek engineering texts and actually re-created Greek mechanical figures. Other mechanical creations from da Vinci include a mechanical clock, a moveable gamecock, and a small organ. In addition to building these devices, he drew hundreds of inventions and included them in his books. Unfortunately, most drawings never became a reality. The the anatomical diagrams in his books remain as evidence that he wanted to re-create the human form. Da Vinci showed an interest in the inner working of the human body, by studying ligaments, tendons, muscle, and bone structure, and how everything interacted to create human movement. His studies of mechanisms and anatomy were precursors to the initial concept of a humanoid robot [6].

There were other pioneering craftsmen who built moveable figurines. The Cittern Player, a movable 17 inch figurine, resembles a small female, with the mechanisms made of wood and iron, and it was covered with cloth. When operating, it appears to mimic bipedal locomotion by way of a small wheel attached to the feet. Additionally, its arms appear to strum a cittern while the head turns. See Figure 1-1. Similar figurines were made by the Swiss and Japanese craftsmen, both allowing a small human statue to move and mimic human movement [6].

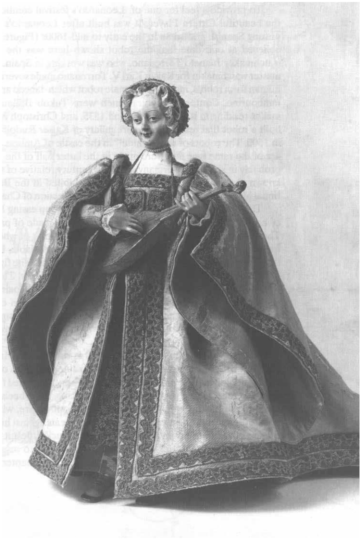

Figure 1-1: The Cittern Player.

The above mentioned “mechanical statues” and mechanisms are the precursors to modern humanoid robots. Even though these figurines could move fingers, open and close their mouths, or even mimic bipedal locomotion, none were anything more than a mere entertainment piece. No one had envisioned the true possibilities of a “mechanical statue,” until the Czech playwright Karel Capek wrote and released his famous play *R.U.R.* (Rossum's Universal Robots) from 1920-1923. This play was the first mention of the word *robot*, conceived from the Czech word *robota*, or slave labor. Capek understood the possible applications of these “mechanical statues,” and in the play the robots were designed as artificial slaves. They eventually overtake their human creators by revolting, resulting in the demise of the entire human race [1].

Although the idea for the slave robot existed since the early 1920's, robots were limited to science fiction. This began to change during the modern industrial revolution, particularly WWII, which brought about many advances in electro-mechanical systems. The first entrepreneurs to develop and market robots were George Devol and Joe Engelberger. Their factory robot was the *Unimate*, the first automotive assembly line robot, and their company pioneered the industrial robotics industry. Later, advances in artificial intelligence, control theory, and manufacturing led to the development of the advanced robotic systems we know today [7].

Capek was indeed a visionary. So much so, that today's state of the art humanoid robots, 80 years after the idea was conceived, can not do many of the tasks in *R.U.R*. Many universities, companies, and even individuals, are currently working on humanoid robots or an important aspect of them. The reason that these robots can not achieve the goals once thought possible in *R.U.R.* is simply because of the level of difficulty. Menzel speaks about the current state-of-the-art in robotics, “We had seen a number of very advanced robots, but most worked haltingly, and some only after interminable delays”[1:16].

The goal of robotics is, “to build and realize humanoid robots, artificial men equipped with proper intelligence capable of operating autonomously, thus replacing trained individuals for dexterous jobs"[8:66]. Humanoid robots will eventually become home robots or personal robots. There is even some speculation that a soccer match will take place 50 years from now with humanoid robots playing against the actual world champions [8].

While the technical aspects of humanoids will one day be realized, how will the robots gain social acceptance? How will people interact with humanoid robots? Will they be afraid of them? Researchers at Vanderbilt University conducted a study and concluded that humanoid "robots will eventually become a part of our daily lives" [9:894]. They suggest that "successful integration" will be achieved after the following conditions must be met: human-like sensors similar to ears and eyes, human-like mannerisms, intelligent decision mechanisms, and natural interaction [9]. Swinson and Bruemmer, researchers at DARPA and Strategic Analysis, Inc., claim, "Ultimately, humanoids might prove to be the ideal robot design to interact with people. After all, humans tend to naturally interact with other humanlike entities" [10:12].

1.2 Literature Review

Current state of the art humanoid robotics research is being conducted in many different areas in locations throughout the world. Because humanoid robotics involves so many different disciplines, every facet cannot be covered in this thesis. Instead, a general overview of the current research and recent advances will be discussed.

Full humanoid robot projects are currently underway at many universities and research institutions. Perhaps the most well known humanoid robots are from Honda R&D Corp., a subsidiary of Honda Motor Corp. Honda has been researching and developing humanoid robotics since 1986. They believe that household domestic robots will be useful in the future and that a humanoid robot is an ideal form to move around domestic locations and obstacles [11]. This means that humanoids are ideal for home servants. Their latest robot, *P3*, shown in Figure 1-2, has 30 degrees of freedom (DOF): six in each leg, seven in each arm, and two for each gripper. A goal of Honda was to improve bipedal locomotion. In addition, other goals were accomplished: walking on normal, even surfaces such as tile, ability to pass through narrow openings, ability to straddle steps and mounds, the ability to walk up staircases, and the ability to walk up a slope. Dexterous manipulation goals included the ability to grasp and hold objects and the ability to perform light work with the dexterous hands via remote control [11].

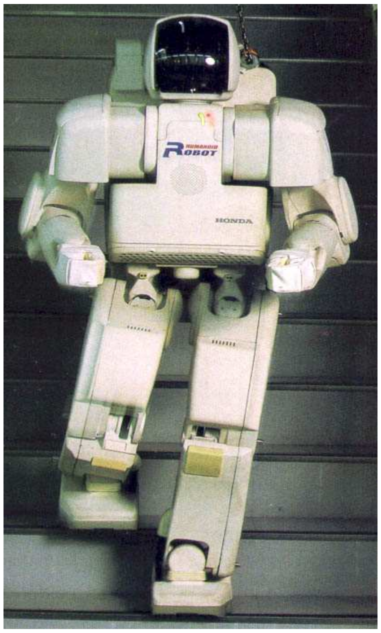

Figure 1-2: Honda's humanoid robot, the *P3.*

Other universities are also developing bipedal humanoid robots. Tohoku University, in Japan, designed and built a 30 DOF humanoid, *Saika-3*. Their primary objective was to develop a lightweight humanoid robot that could be easily handled by a person [12]. Another lightweight humanoid robot was constructed at Monash University in Australia. The researchers selected polyurethane plastic as their building material, indicating that "it is an ideal material for indoor robotics" [12:1571]. The *Monash Man*, as the researchers call it, has 43 DOF. Their long-term humanoid robotics research will focus on humanoid motion, sensory perception, control systems, and human-robot interaction [13]. *WABIAN-RII* is the name of a humanoid robot designed and built at Waseda University in Japan. This robot also has 43 DOF, and its primary goal is to mimic human-like motion, even expressing emotion by its particular gait [14].

The above-mentioned humanoids are attempts to recreate the complete human form. However, some researchers have opted to concentrate on the upper torso, developing new and improved control techniques for robotic arms, dexterous robotic hands, and active stereo vision heads. The following projects are not complete humanoids, rather some portion of them, typically the upper torso.

The National Aeronautics and Space Administration (NASA) has undertaken an ambitious project to develop *Robonaut*, a space humanoid that will be used for teleoperation in space. The humanoid form is ideal because it can use the same tools and work in the same space that was designed for an astronaut. The NASA researchers have focused on the upper torso, designing an arm and head that has more thermal endurance, sensing, strength, and more dexterity than any current system [15]. The NASA researchers claim that, "Unlike humanoid robots now being developed for entertainment or as technical curiosities, *Robonaut* will actually perform work" [15:57]. See Figure 1-3.

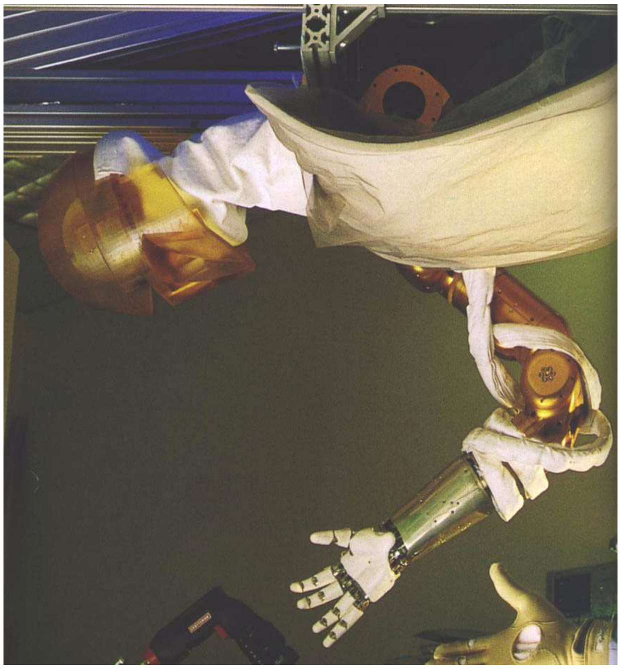

Figure 1-3: NASA's humanoid robot, *Robonaut.*

Researchers at the Electrotechnical Laboratory in Japan developed a "high strength" upper torso, using high performance actuators that allow the robot to do push-ups. They claim that most of the previous work assumes that the upper torso of a humanoid robot is supported by the lower torso and that the robot's main objective is to gesture in free space, which they feel is false. Therefore, they are developing new control techniques to "exploit redundant degrees of freedom, strong dynamics, and global dynamic structures inherent in each task situation and achieving these tasks in the presence of uncertainty" [16:1578]. See Figure 1-4.

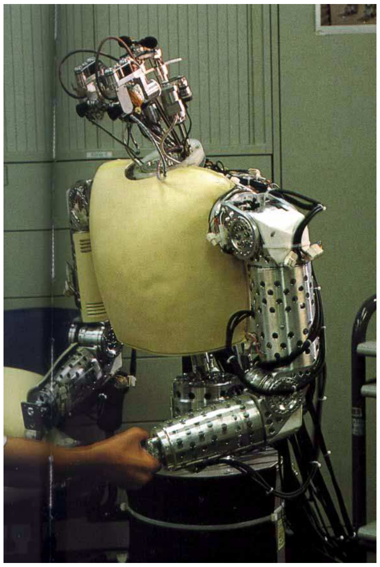

Figure 1-4: Electrotechnical Laboratory's robot, the *ETL-humanoid.*

While many full humanoids use bipedal locomotion, some have been developed that use wheels for mobility. A robot developed at Waseda University called *WENDY* (Waseda Engineering Designed sYmbiont) has four drive wheels. The researchers claim that a true symbiot (a humanoid robot that interacts with people) must not be bipedal, and bipedal research is "not applicable to the human symbiotic robots directly" [17:3183].

The above mentioned humanoid systems are attempts to recreate autonomous systems. However, some researchers feel that humanoid systems do not have to be autonomous. Lee et al.

developed a teleoperated master-slave humanoid robotic arm system that accurately senses the master operator's arm position and can provide force feedback. They accomplished this by using pneumatic actuators embedded in the master control arm and explained that “Human[s] can feel virtual volume in [their] hand with force reflection” [17:2576]. They also state that force feedback is required to achieve complex tasks of manipulation [17].

Biologically inspired actuation methods have been developed. Researchers at the University of Salford, in England, created a humanoid robot using pneumatic Muscle Actuators (pMAs). These actuators are designed to mimic the effects of human muscle tissue. They are lightweight, compliant, and have a very high power to weight ratio, making them ideal for an autonomous humanoid robot. The pMAs are arranged in antagonistic pairs for each degree of freedom, allowing stiffness control of each joint. This allows for more human-like movement. Overall, their robot was a successful attempt to create a “biomimetic” humanoid due to the implementation of muscle-like actuators [19]. See Figure 1-5.

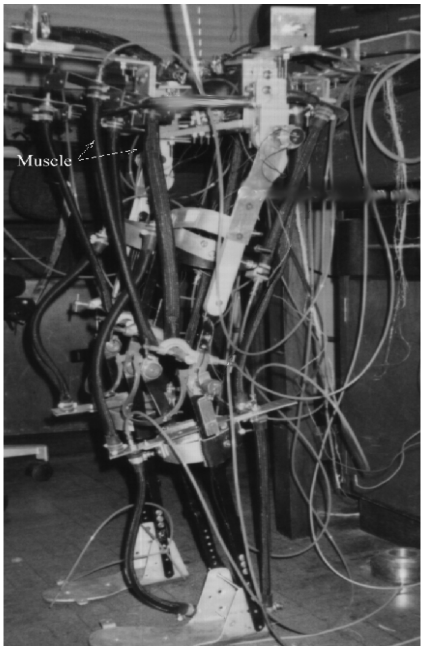

Figure 1-5: Pneumatically actuated humanoid robot.

Advances in biomimetic learning algorithms were made possible by the use of humanoids. Taddeucci, Dario, and Ansari, from the ARTS Laboratory in Italy, state, “a robot endowed with a means to perceive external events and a cognitive system able to process the perceived data to dynamically accomplish a particular task (in other terms a “humanoid”), provides the necessary substrate for a serious exploration of body-based intelligence hypothesis” [20:537]. Their end goal was to have a humanoid robot interact with humans in an everyday environment with minimal impact. Implementation of various machine learning techniques such as neural networks and synthetic psychology coupled with a humanoid robot provided insight about the best way to teach natural human-humanoid interaction [20].

Research on efficient control and computation of inverse kinematics for humanoid robots was conducted at the University of Southern California. Because humanoid robots have so many degrees of freedom, an efficient inverse kinematic solution is needed. Their paper examines two common techniques, the pseudo-inverse with explicit optimization and the extended Jacobian method. Their claim is that pseudo-inverse methods are a more efficient choice when determining the inverse kinematics of a humanoid robot. Their results were tested on a 30 DOF humanoid robot with promising results; they concluded that the pseudo-inverse method had much better convergence then the other methods [21].

Computer vision research continues to extend the vision capabilities of humanoid robots. A common arrangement consists of an active stereo head with two cameras. Yamato developed a control system for a humanoid robot, named *Cog,* based on infant eye development. The task of tracking an object was divided into three sub-tasks: ocular alignment, sensory binocularity, and convergence. They successfully implemented the sub-tasks as individual modules, and then the modules were combined to permit object tracking. The entire control system was shown to track objects on an active stereo head [22].

While many researchers have focused on development of humanoids, the systems required for motion, and the artificial intelligence aspect, a group of researchers at MIT are using humanoids as tools for testing developmental psychology and cognitive science. They are applying psychological theories to humanoid systems to test their hypotheses. They want to implement psychological theories on humanoids and see how accurately the theories mimic humans [23].

1.3 This Work

A humanoid robot, *Omnibot 2000*, was developed at the University of Florida's Machine Intelligence Laboratory (MIL) in the summer of 1999. *Omnibot* is not a full humanoid, however, it consists of an upper torso with a head, neck, two arms, all resting on a mobile base. Each arm has five degrees of freedom, including a gripper as an end-effector. The robot also has two degrees of freedom for the head, allowing it to pan and tilt. Additionally, the base contains six drive wheels. The robot has a total of 12 degrees of freedom; each actuated by a servo. The wheeled base also has two drive motors, each rotating a pair of wheels on each side of the robot. It is 30 inches tall, 24 inches wide and 15 inches deep [24]. See Figure 1-6.

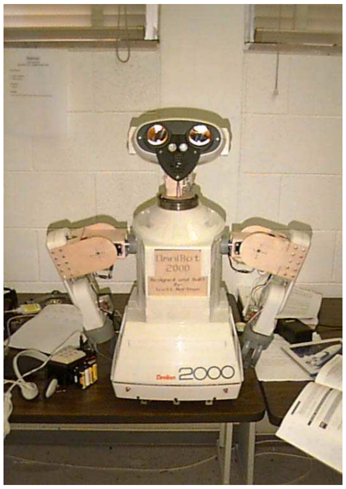

Figure 1-6: MIL’s first humanoid, Omnibot 2000.

Omnibot is designed to be a personal assistant, capable of helping the elderly or disabled. Additionally, *Omnibot* can entertain and perform. Behaviors include obstacle avoidance, wall following, obeying commands, and performing. The user determines the behaviors via *Omnibot's* voice recognition system. Commands are issued to *Omnibot*, and it responds by repeating the words, and performs the specified behavior. *Omnibot* contains four different sensor suites, including infrared emitters and detectors, bump switches, voice recognition, and low-resolution vision. During wall following behavior, *Omnibot* will turn away from objects in its path. When it is doing wall following, it will follow the walls of a room, and it will also avoid bumping into obstacles. When *Omnibot* is in its "obeying commands" behavior, the user can instructs it to move the arms, grippers, head, and body; *Omnibot* is a slave, performing any tasks the user requests. When it is told to dance, it will start singing and dancing to *The Village People's "*YMCA", or any other song programmed.

Due to the success of the Machine Intelligence Laboratory's (MIL) *Omnibot* project, another humanoid project was started. The new robot, called *Pneuman*, is currently being designed and developed at the University of Florida's MIL. *Pneuman* will be a more advanced version of *Omnibot* and it will interact with the world by means of a voice synthesizer and voice recognition. Additionally, there will be a text user interface to adjust *Pneuman's* parameters and control its joints.

Pneuman's primary purpose is to advance humanoid research. Areas of interest include artificial cognition, natural language processing, active stereo vision, path planning, autonomous navigation, inverse kinematics, manipulator control, and human-humanoid interaction. This thesis discusses the details regarding the design, construction and control of *Pneuman*. Chapter 2 explains the details regarding the physical aspects of *Pneuman*, including the size of the structure, the degrees of freedom, the drive system, and the kinematics. Chapter 3 details the electronic systems on *Pneuman* including the power system, the computer system, the custom electronics, and the sensor systems. Chapter 4 talks about the control theory and trajectory generation techniques

Pneuman uses. Chapter 5 illustrates the text user interface used for development. Chapter 6 concludes by suggesting future areas of work. See Figure 1-7 for a computer aided design (CAD) rendering of *Pneuman*.

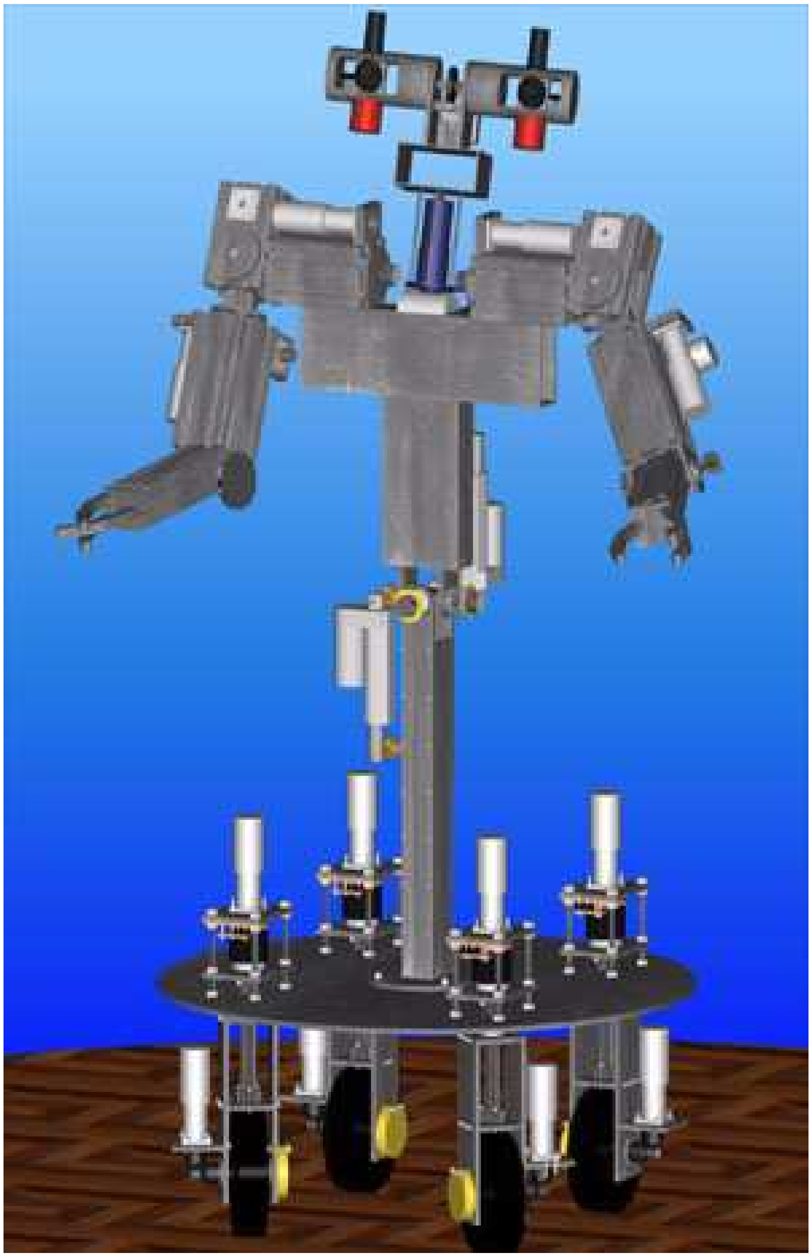

Figure 1-7: University of
Florida's humanoid, *Pneuman.*

CHAPTER 2
PHYSICAL STRUCTURE

2.1 Overall Design Considerations

The overall goal of building *Pneuman* is to develop a platform that has several useful attributes conducive to humanoid robot research. In addition to research, the robot will give guided tours of the MIL. Other possible uses include entertainment and operation as a personal assistant. Due to these requirements, a humanoid platform was ideal.

A humanoid robot provides many areas for research. The two main areas can be classified as artificial intelligence and control. Artificial intelligence may be divided further into human-robot communication, path planning, machine learning, machine vision, and cognition. The overall control area may be divided into kinematics and dynamic systems control. The areas that will be discussed in this paper include kinematics and dynamic systems control.

Natural human-robot communication will be possible with verbal interaction. A speech recognition system combined with a natural language processing system will allow *Pneuman* to understand simple phrases and respond verbally with a voice synthesizer. *Pneuman* will navigate throughout its environment using a verity of sensors, including sonar, infrared emitter/detector pairs, bump switches, and optical encoders. The sonar and infrared sensors will provide the robot with obstacle distance information. The bump switches will signal to the robot that an obstacle was contacted. Finally, the robot can use dead-reckoning to estimate the amount of distance traveled with the optical encoders. This information is processed by *Pneuman's* computers and used to compute the possible paths it may take to move from one point to another.

Machine learning techniques will be used to improve the kinematics for the position if the end effectors, as well as positioning the drive wheels. The techniques will compensate for any unmodeled effects such as machining tolerances, backlash, flexing, friction, etc. An advantage of using these techniques is that the kinematic and dynamic models are simpler. A disadvantage is that the systems must be trained. However, the benefits outweigh the disadvantages.

Pneuman's vision system will also use machine learning techniques to identify objects in an image. Color models of objects will be generated and stored in *Pneuman's* computer. When an object is identified in the stereo images, *Pneuman's* active stereo head will focus onto the objects, and each eye will converge to center the object in the field of view. The disparity between the eyes will provide *Pneuman* with information about the location of the object in space. *Pneuman* can then use this information to position its end effectors in the proper location, possibly to pick up the object.

Cognition is defined as, “The act or process of knowing” by *Webster's Dictionary* [25:156]. Many researchers throughout the world are currently trying to make robots that “know” things or “think.” Some claim that it is an impossible task, while others feel that it can be done in the future. But the most advanced artificial intelligence today still falls short of anything portrayed in science fiction. Consequently, *Pneuman* will not be able to “know” everything, but it will have the ability to carry out specific tasks. *Pneuman* will be programmed to talk and demonstrate its abilities, or it may be programmed to grab a soda from a cooler. Whatever the programs are, ever so trivial by human standards, *Pneuman* will be an excellent platform for many types of artificial intelligence research.

Additionally, when *Pneuman* gives tours of the MIL, its humanlike appearance, humanlike motions, gestures, and communication should enhance the overall impact of the robot. People should feel comfortable interacting with *Pneuman* due to the humanlike structure. The eyes will wander around similar to a human's eyes. While speaking, natural gestures and motions should enhance *Pneuman's* verbal communication ability. The arms will point at objects of interest just as humans do. The articulated waist allows *Pneuman* to bend over, as if it were picking an object up from the floor. Finally, the maneuverable base will allow *Pneuman* to translate in any direction and rotate about any point. All of these features contribute to *Pneuman's* overall ability to give tours and entertain an audience.

Due to *Pneuman's* humanoid form, it will also make an ideal personal assistant. *Pneuman* can use the five joint articulated robotic arms and end-effectors to reach for and grasp objects. The natural communication interface will allow a user to issue verbal commands to *Pneuman*, instructing the robot to perform any needed tasks. The highly maneuverable base is ideal for a cluttered area, such as a home, where a personal assistant may be needed.

2.2 Specifications

2.2.1 Overall Size

Pneuman stands approximately 59 inches tall, measured from the bottom of the drive wheels to the top of the stereo head. The widest points are from shoulder to shoulder and across the base, both measuring 26 inches across. Each of the five DOF arms allows *Pneuman* to grasp objects approximately twenty inches away. The base consists of the lower 29 inches of the robot, while the rest is the upper torso. See Figure 2-1.

2.2.2 Weight

The overall weight of the structure is a primary concern because *Pneuman* is an autonomous robot. Therefore, the power source for all electronics and actuators are carried on-board and no external power may be used. While efficient control and motor operation techniques are utilized, an ideal way to ensure a long battery life is to minimize the weight of the robot. The weight-minimized configuration was not conceived initially; previous revisions called for a much bulkier structure as shown in Figure 2-2. The final design removed much of the material covering the wheels, and removed the unnecessary circular platform of the base.

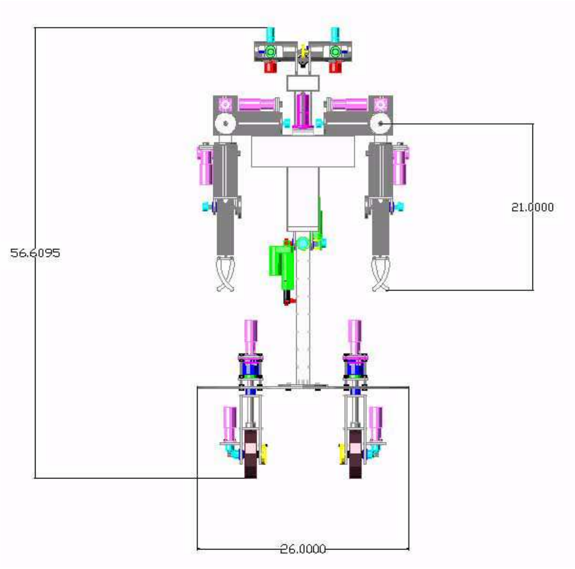
56.6095
21.0000
26.0000

Figure 2-1: *Pneuman's* overall dimensions.

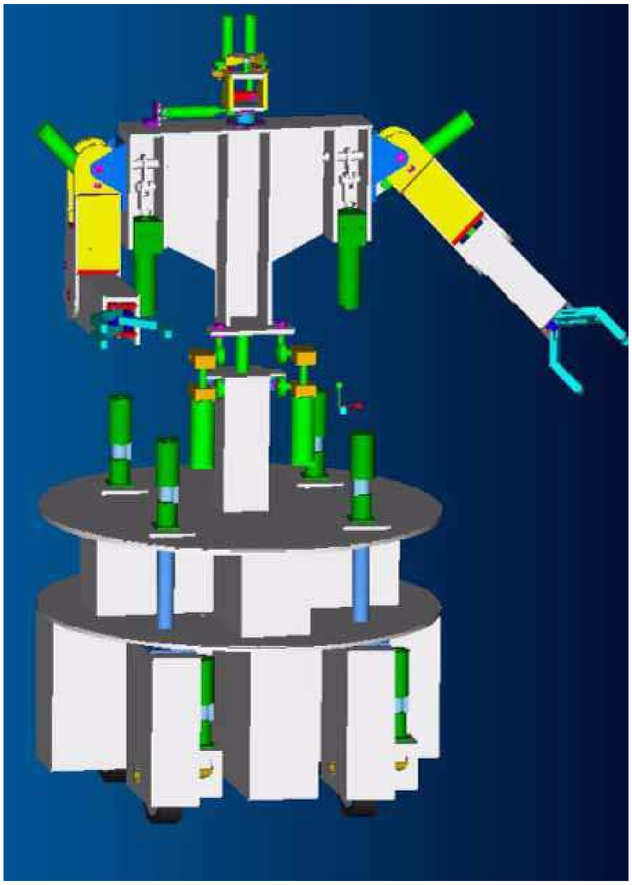

Figure 2-2: *Pneuman's* original design.

The entire robot weighs approximately 102 pounds. A major portion of the weight may be attributed to the four sealed lead acid batteries, each weighing approximately 10 pounds. *Pneuman's* base weighs approximately 25 pounds (excluding the batteries), the upper torso weighs approximately 30 pounds (including the five DOF arms), and the head weighs approximately seven pounds.

2.2.3 Mobility

In terms of mobility, the goal was to give *Pneuman* access to the same areas humans live and work in. Two main locomotion options included a wheeled base or a legged walking mechanism. The wheeled base is more efficient for accomplishing a given task, and it simplifies the overall design considerably. While a legged mechanism offers some advantages over rough terrain, *Pneuman* will primarily travel over smooth surfaces. Due to these constraints, a wheeled drive base is used. The wheeled drive base is explained in detail in a later section.

2.2.4 Degrees of Freedom (DOF)

The human body has over 40 DOF. While *Pneuman* attempts to mimic the human form, simplifications were made to ensure autonomous real-time control. Therefore, *Pneuman* has 25 DOF. To accomplish the humanlike motions, two five DOF arms will be used. Each arm will have a gripper as an end-effector. In addition to the arms, *Pneuman* will have an active stereo head, containing two cameras, with three DOF. Each camera may be considered and “eye.” Both eyes will tilt together, while each eye can converge independently. The head will sit on a two DOF neck, allowing the entire head to pan and tilt. The entire upper torso connects to the wheeled base via a two DOF waist. The waist will allow the upper torso to tilt front to back and side to side. Finally, *Pneuman's* base moves via four drive wheels, each wheel steering independently, giving *Pneuman* maximum maneuverability.

2.3 Drive System

2.3.1 Overview

Pneuman's base contains four drive wheels arranged in a square. Each wheel is capable of steering independently, known as a modified-synchronous drive system. This gives *Pneuman* maximum maneuverability. The drive system can operate in three different steering modes; “skid-steer”, Ackerman, and four-wheel or "crab" steer. While crab steering is primarily used, each has advantages and disadvantages that will be explained in later sections.

The wheels are approximately six inches in diameter, 13 inches apart. The wheels pivot about their center line and have an operating range of 180 degrees. Each wheel and steering mechanism is geared to a 485 oz.-in. planetary gearhead motor, providing adequate torque. The maximum velocity of the motors is approximately 45 r.p.m., permitting each wheel to change steering direction at a maximum rate of 180°/1.3s. The given motor/wheel combination also allows *Pneuman* to translate at a maximum rate of 14 in./s.

A quantitative description of motion involves a way to describe the path of the agent and the kinematics of the mechanism required for that motion. A straight path is described by the distance traveled, *d*. An arc of radius r_s and a sweep angle $_s$ may describe a curved path. The kinematics may be determined from simple geometry. The *instantaneous center of curvature (I.C.C.)*, a point where the base’s motion appears to move around, lies where the perpendicular bisectors of each wheel intersect with each other. Any configuration of the wheels that do not allow all of the bisectors to intersect at a common point will cause wheel slippage, resulting in inaccuracies while path planning. See Figure 2-3.

Pneuman has three steering modes: skid, Ackerman, and “crab,” and each mode will be explained in detail in this section. Skid steering is not typically used due to inaccuracies associated with it. Ackerman steering is commonly used on automobiles, and much research has been done on the theory and modeling of this steering configuration.

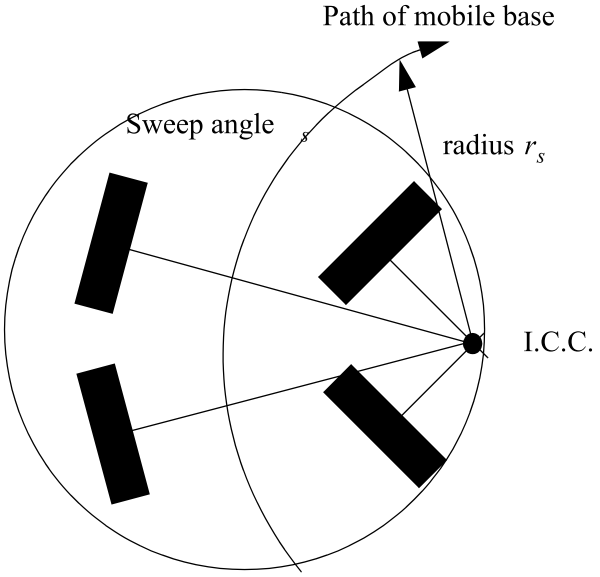

Figure 2-3: The instantaneous center of curvature, *I.C.C*.

However, there are kinematic constraints that limit its use. The final and preferred method is "crab" steering where all wheels are capable of changing their orientation. *Pneuman* will primarily use this method of steering.

2.3.2 Skid Steering

Many wheeled robots use "skid steering". This simply means that the orientation of each drive wheel is fixed, and turning is made possible by varying the speed of each side's drive wheels with respect to the other side. This is an effective and easy solution to steering the robot. However, it is not as accurate as other steering methods; certain characteristics including friction, wheel slippage, and other unpredictable attributes cause problems [26]. This steering configuration is a special case where the bisectors of the wheels do not intersect and the fact that the wheels slip is exploited to cause the robot to rotate. See Figure 2-4.

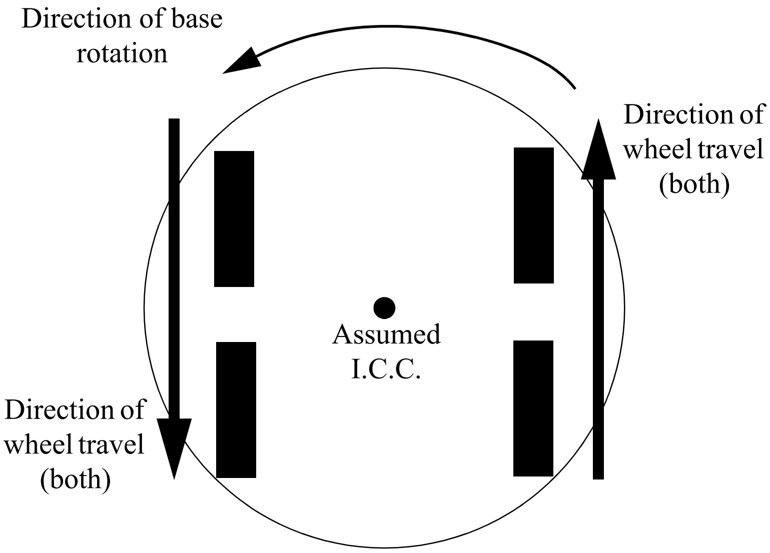
Direction of base rotation
Direction of wheel travel (both)
Assumed I.C.C.
Direction of wheel travel (both)

Figure 2-4: Skid steering. Note that the perpendicular bisectors do not intersect, and the I.C.C. is not exactly known.

2.3.3 Ackerman Steering

This type of steering is used in most automobiles.The two rear wheels remain at a fixed orientation, facing towards the front of the vehicle.This means that the perpendicular bisector is the same for both rear wheels, extending in a line away from the vehicle. The two front wheels change their steering angle to steer the vehicle. Note that the steering angle for each of the front wheels is different to insure that their perpendicular bisectors intersect at the same point along the rear wheel perpendicular bisector. See Figure 2-5.

2.3.4 Four-wheel Steering

Four-wheel, or “Crab” steering, has the same requirement as Ackerman steering; all of the wheel's perpendicular bisectors must intersect at a common point to avoid wheel slippage. In this mode, however, all of the wheels are allowed to change orientation. This means that the *I.C.C.* can be anywhere, not just along the mutual perpendicular of the rear wheels as in Ackerman steering.

A major advantage of this mode is that the turning radius can vary from zero to infinity, and it can lie anywhere in the plane of motion. See Figure 2-6.

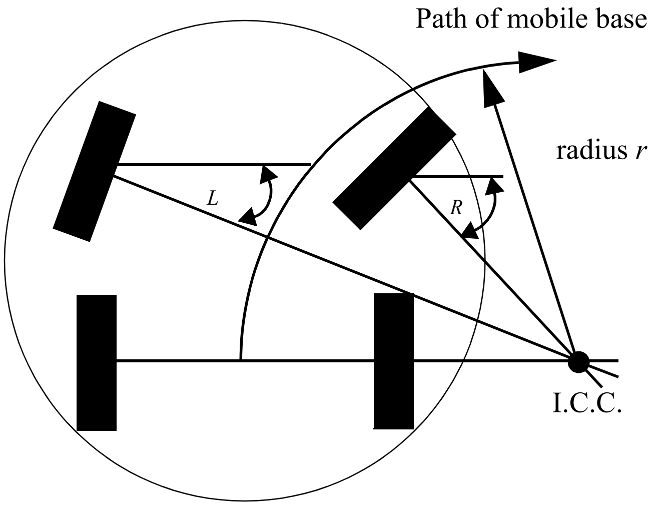

Figure 2-5: Ackerman steering. Note that the I.C.C. lies along the mutual perpendicular bisector of the rear wheels.

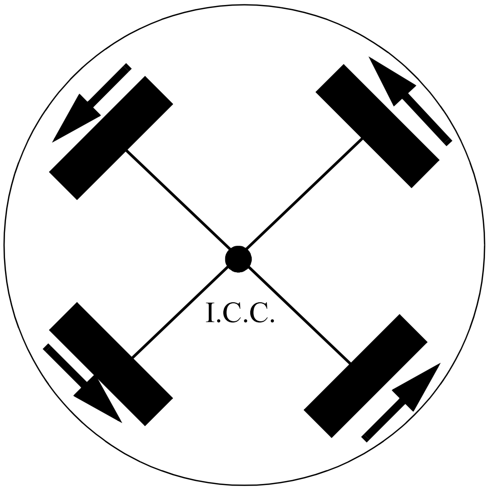

Figure 2-6: Four-wheel or “crab” steering. Note that all four wheels are turned, and the I.C.C. is the center of the base.

2.3.5 Physical Implementation

The base assembly consists of a round aluminum plate with four drive wheel assemblies mounted in a circular arrangement. The large aluminum plate provides mounting space for all of *Pneuman's* batteries, power supplies, computers, sensors, and the waist assembly. See Figure 2-7.

Each drive wheel assembly contains two motors; one for steering the drive wheel and one for rotating the drive wheel. The steering motor has an operational range of 180 degrees. This is limited by the wires for the drive motor and for the optical encoder. A limit switch is integrated into each steering assembly to insure that the operational range is not exceeded, which may damage the wires. See Figure 2-7.

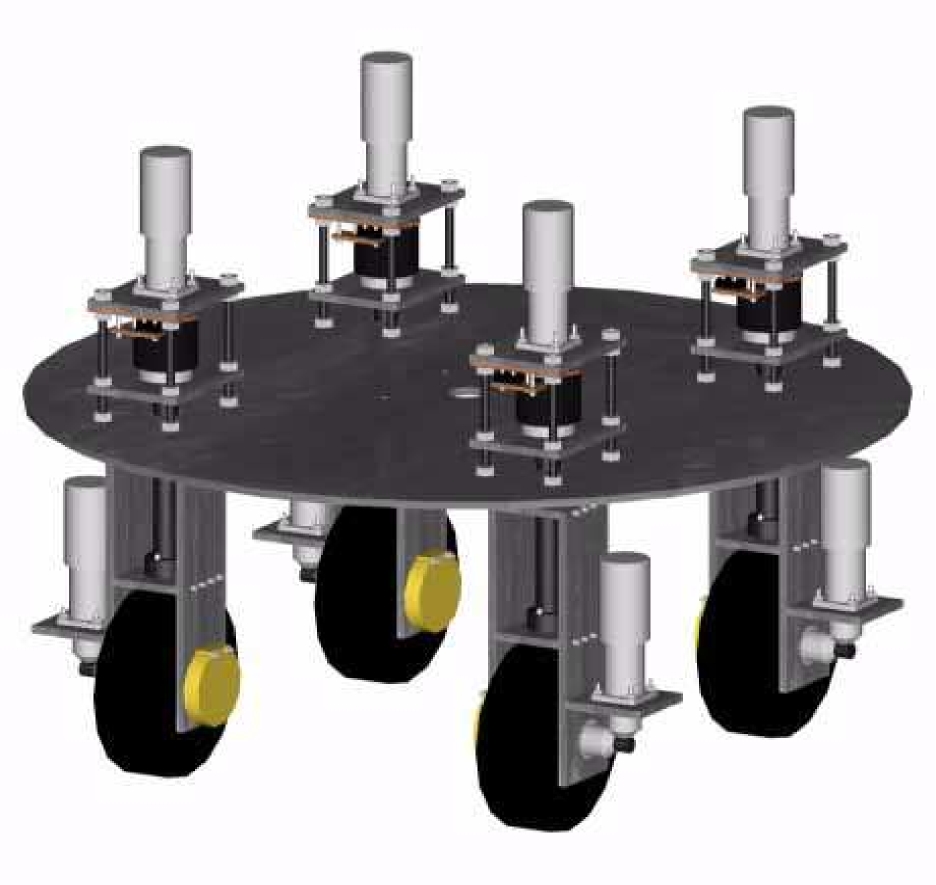

Figure 2-7: The base and wheel assemblies.

2.4 Kinematics

2.4.1 Active Stereo Head Design Considerations

Pneuman's vision system consists of a four DOF stereo head with convergence, tilt, and pan. These DOF are needed to allow *Pneuman* identify the location of an object in a 3D space. Each eye can move independently, allowing each camera to converge on to an object. Additionally, each eye uses an optical encoder providing an angular resolution of 0.036 degrees. This will allow *Pneuman* to determine the location of objects with high accuracy. See Figure 2-8.

The geometry required to determine the location of an object with the stereo head is illustrated in Figure 2-9. Each eye will be able to determine the object of interest using computer vision techniques. After the centroid of each object is determined, each camera will converge on the object such that the center of the image will correspond to the centroid of the object. The disparity between the camera angles, $_L$ and $_R$, will allow *Pneuman* to know the location of the object in 3D space.

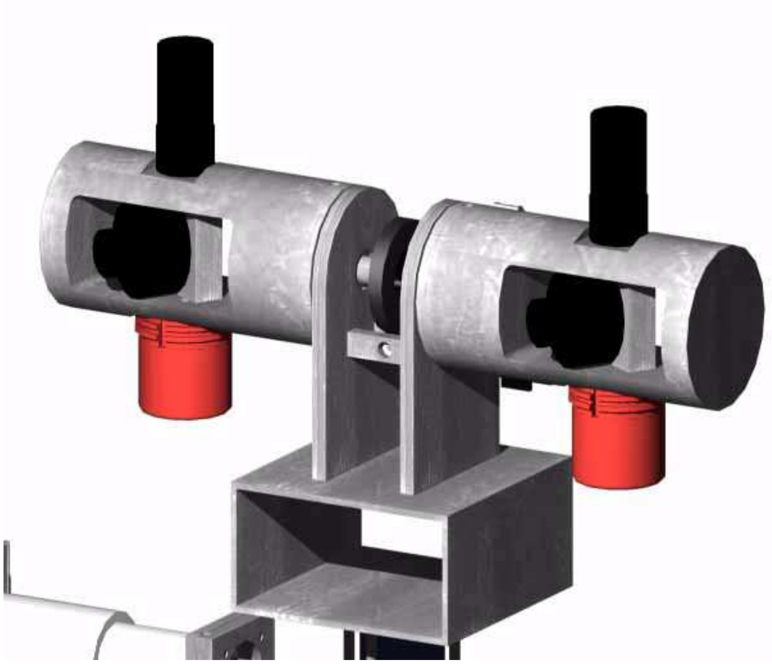

Figure 2-8: *Pneuman's* active stereo head.

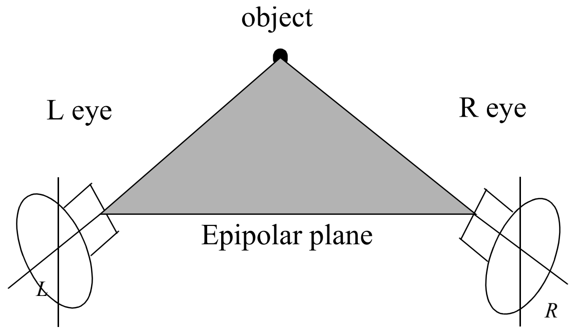

Figure 2-9: Epipolar plane formed by two cameras and the object.

2.4.2 Robotic Arm Design Considerations

The two arms discussed below are five degree-of-freedom (5 DOF) serial link manipulators. Constructed entirely from aluminum, the arms were designed to perform tasks similar to human arms. Upper and lower arm lengths are proportional to that of an adult human. Explosion of kinematics equations were kept to a minimum by aligning the axes of rotations from joint to joint as shown in Figure 2-10. The arms are mirror images of each other and are identical in all other respects [27].

When designing a serial link manipulator, one must consider the kinematics equations behind each joint placement. The arm was designed so that joint axis i intersects joint axis $i+1$, where i is the number of joints in the arm. Each new link is offset from the previous link by 90 degrees as shown in Figure 2-11. See Table 2-1 for joint characteristics [27].

Joints ShoulderA, ShoulderB, and ShoulderC are coincident at the shoulder. This alignment allows for the arm to rotate as if a ball and socket joint were implemented. The Elbow and Wrist joints are also coincident. All joints are actuated by planetary gearhead motors [27]. The forward and inverse kinematic solutions are straightforward due to the fact that the principal axes of all the joints are aligned. Figure 2-12 shows the coordinate frame assignments.

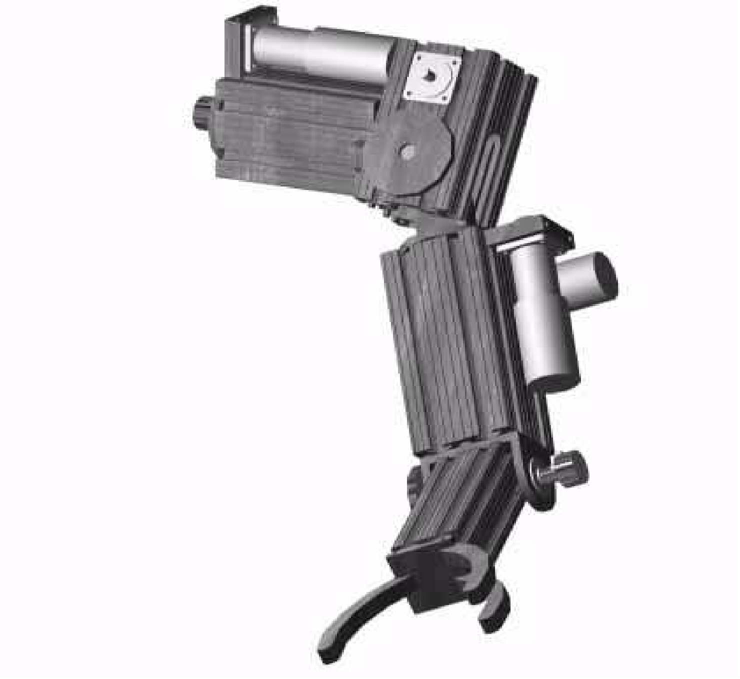

Figure 2-10: One of *Pneuman's* robotic arms.

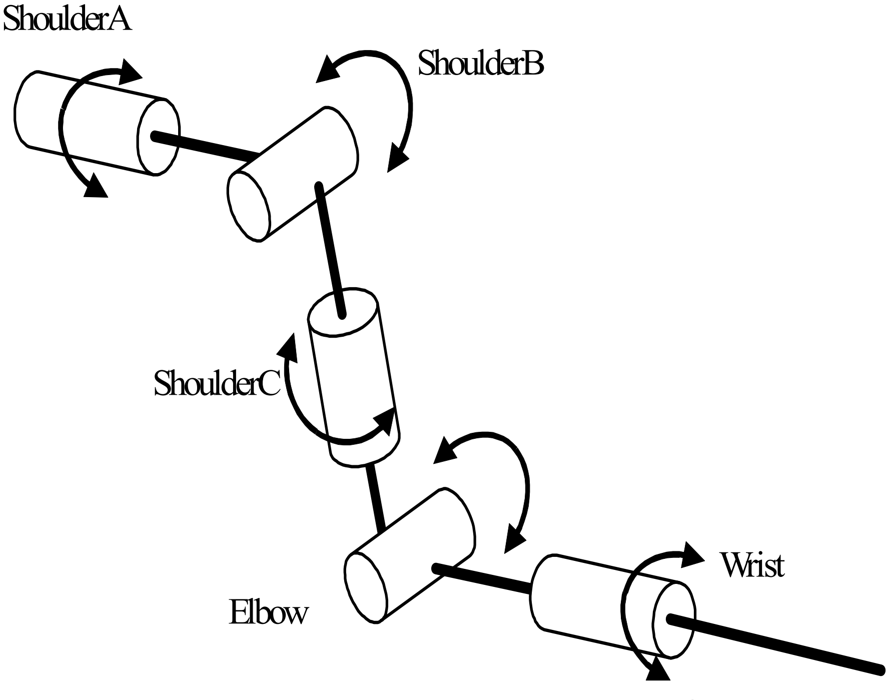

ShoulderA
ShoulderB
ShoulderC
Elbow
Wrist

Figure 2-11: Kinematic representation of *Pneuman's* arms.

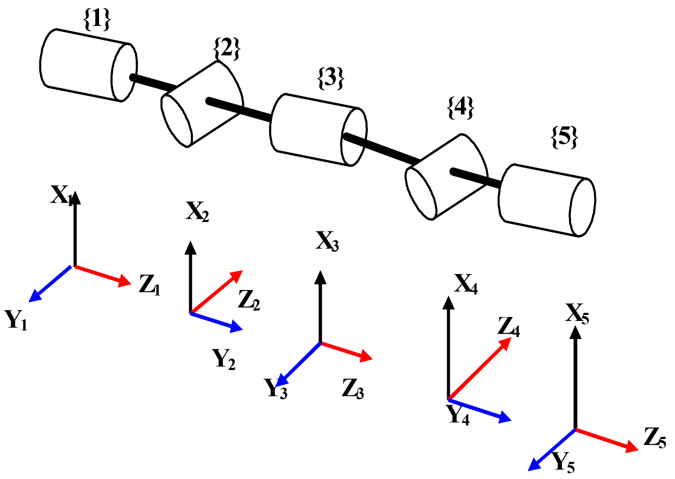

Figure 2-12: Coordinate frame assignment for arms.

Note that frame {0} is coincident with frame {1} when $_1$ = 0. The DH parameters are shown in the table below.

Table 2-1: D-H Parameters for 5 DOF Arm

I	$_{I-1}$	a_{i-1}	d_i	$_i$
1	0	0	0	$_1$
2	$\frac{}{2}$	0	0	$_2$
3	$-\frac{}{2}$	0	d_3	$_3$
4	$\frac{}{2}$	0	0	$_4$
5	$-\frac{}{2}$	0	0	$_5$

Note the base frame {0} is positioned at the shoulder. This is the arm's point of attachment to the body of *Pneuman*. The origin of frame {5} is located at the wrist. A dexterous hand may be attached here in the future [27].

The overall forward kinematics of the manipulator, derived from the DH parameters, is given by the transform (Note: $c_x = \cos \quad _x$ and $s_x = \sin \quad _x$, where $\quad _x$ refers to the position of joint *x*.)

$$ {}^{0}_{5}T = \begin{bmatrix} r_{11} & r_{12} & r_{13} & p_x \\ r_{21} & r_{22} & r_{23} & p_y \\ r_{31} & r_{32} & r_{33} & p_z \\ 0 & 0 & 0 & 1 \end{bmatrix} \qquad (2\text{-}1) $$

where

$$ r_{11} = c_5 \ \ c_4 \ \ c_1c_2c_3 - s_1s_3 \ \ - c_1s_2s_4 \ \ - \ \ c_3s_1 + c_1c_2s_3 \ \ s_5 \qquad (2\text{-}2) $$

$$ r_{12} = -c_5 \ \ c_3s_1 + c_1c_2s_3 \ \ - \ \ c_4 \ \ c_1c_2c_3 - s_1s_3 \ \ - c_1s_2s_4 \ \ s_5 \qquad (2\text{-}3) $$

$$ r_{13} = -c_1c_4s_2 - \ \ c_1c_2c_3 - s_1s_3 \ \ s_4 \qquad (2\text{-}4) $$

$$ p_x = -d_3c_1s_2 \qquad (2\text{-}5) $$

$$ r_{21} = c_5 \ \ c_4 \ \ c_2c_3s_1 + c_1s_3 \ \ - s_1s_2s_4 \ \ - \ \ c_2s_1s_3 - c_1c_3 \ \ s_5 \qquad (2\text{-}6) $$

$$ r_{22} = -c_5 \ \ c_2s_1s_3 - c_1c_3 \ \ - \ \ c_4 \ \ c_2c_3s_1 + c_1s_3 \ \ - s_1s_2s_4s_5 \qquad (2\text{-}7) $$

$$ r_{23} = -c_4s_1s_2 - \ \ c_2c_3s_1 + c_1s_3 \ \ s_4 \qquad (2\text{-}8) $$

$$ p_y = -d_3s_1s_2 \qquad (2\text{-}9) $$

$$ r_{31} = c_5 \ \ c_3c_4s_2 + c_2s_4 \ \ - s_2s_3s_5 \qquad (2\text{-}10) $$

$$ r_{32} = -c_5s_2s_3 - \ \ c_3c_4s_2 + c_2s_4 \ \ s_5 \qquad (2\text{-}11) $$

$$ r_{33} = c_2c_4 - c_3s_2s_4 \qquad (2\text{-}12) $$

$$ p_z = d_3c_2 \qquad (2\text{-}13) $$

where d_3 is the distance between ShoulderB (frame {2}) and ElbowA (frame {3}) and that the origin of the frame for ElbowA is the same as the origin of the frame for ElbowB (frame {4}) [27].

After the forward kinematics solution was determined, the closed form inverse kinematic solution was found for the 5 DOF arm. The solutions for the joint angles are

$$ {}_1 = \mathrm{atan2}\ \ -p_y\ \ -p_x \tag{2-14}$$

$$ {}_2 = \mathrm{atan2}\ \ \sqrt{p_x^2 + p_y^2}\ \ p_z \tag{2-15}$$

$$ {}_3 = \mathrm{atan2}\ \ -r_{12}c_1c_2 + r_{23}s_1c_2 + r_{33}s_2\ \ \ r_{12}s_1 - r_{23}c_1 \tag{2-16}$$

$$ {}_4 = \mathrm{atan2}\ \ \begin{matrix} \sqrt{\ r_{31}c_2 -\ \ r_{11}c_1 + r_{21}s_1\ \ s_2\ \ ^2 +\ \ r_{32}c_2 -\ \ r_{12}c_1 + r_{22}s_1\ \ s_2\ \ ^2\ } \ , \\ r_{33}c_2 - r_{12}c_1s_2 - r_{23}s_1s_2 \end{matrix} \tag{2-17}$$

$$ {}_5 = \mathrm{atan2}\ \ \begin{matrix} c_3\ \ r_{21}c_1 - r_{11}s_1\ \ -\ \ r_{11}c_1c_2 + r_{21}s_1c_2 + r_{31}s_2\ \ s_3\ \ , \\ c_3\ \ r_{22}c_1 - r_{12}s_1\ \ -\ \ r_{12}c_1c_2 + r_{22}s_1c_2 + r_{32}s_2\ \ s_3 \end{matrix} \tag{2-18}$$

2.4.3 Waist Joint Design Considerations

The waist joint kinematics must be considered in addition to the arm kinematics. The waist is a two DOF joint, exactly like a universal joint, providing *Pneuman's* upper torso pitch and yaw movement. As in the arm design, both axes of rotation are aligned to keep the kinematics simple. See Figure 2-13 for a kinematic representation of the waist joint and placement of the reference frames. The D-H parameters for the waist joint are shown in Table 2-2. Note that frame {0} is coincident with frame {1} when ${}_1$ equals zero.

The overall forward kinematic transform is

$$ {}^0_2T = \begin{bmatrix} r_{11} & r_{12} & r_{13} & p_x \\ r_{21} & r_{22} & r_{23} & p_y \\ r_{31} & r_{32} & r_{33} & p_z \\ 0 & 0 & 0 & 1 \end{bmatrix} = \begin{bmatrix} \cos\ {}_1 \cos\ {}_2 & -\cos\ {}_1 \sin\ {}_2 & -\sin\ {}_1 & 0 \\ \cos\ {}_2 \sin\ {}_1 & -\sin\ {}_1 \sin\ {}_2 & \cos\ {}_1 & 0 \\ -\sin\ {}_2 & -\cos\ {}_2 & 0 & 0 \\ 0 & 0 & 0 & 1 \end{bmatrix} \tag{2-19}$$

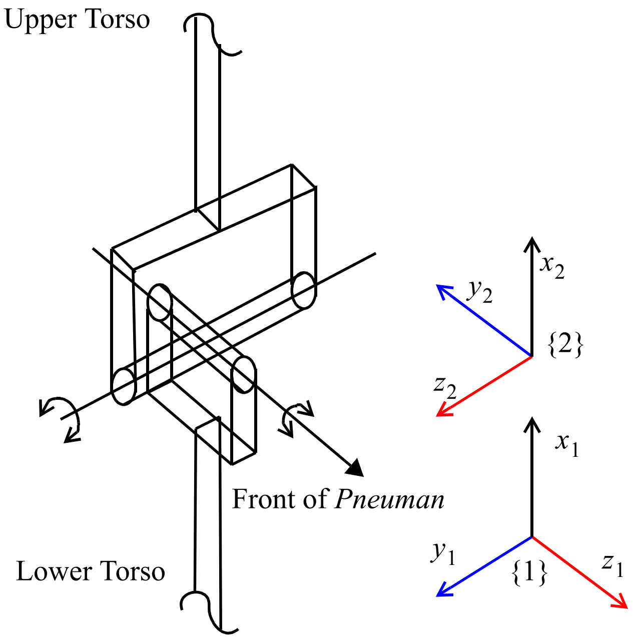
Upper Torso
x_2
y_2
{2}
z_2
x_1
Front of *Pneuman*
y_1
{1}
z_1
Lower Torso

Figure 2-13: Kinematic figure of *Pneuman's* waist joint.

Table 2-2: D-H Parameters for 2 DOF Waist

I	$_{I-1}$	a_{i-1}	d_i	$_i$
1	0	0	0	$_1$
2	$-\frac{\ }{2}$	0	0	$_2$

The closed form inverse kinematic solution for the waist was also determined:

$$_1 = \operatorname{atan2}\ -r_{13}\ r_{23}\ \ , \tag{2-20}$$

$$_2 = \operatorname{atan2}\ -r_{31}\ -r_{32}\ \ . \tag{2-21}$$

A CAD drawing of the waist assembly is shown in Figure 2-14.

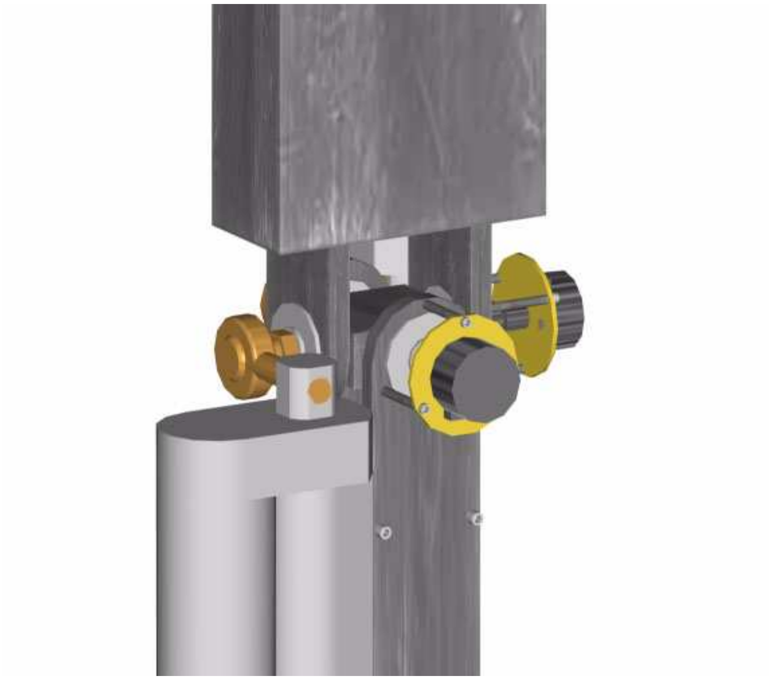

Figure 2-14: *Pneuman’s* waist joint.

CHAPTER 3
ELECTRONIC SYSTEMS

3.1 Overview

While much time and effort was devoted to the mechanical structure of *Pneuman*, it would be a lifeless statue without the electronic systems. *Pneuman's* electrical system consists of four sealed lead-acid batteries, a power distribution block, a regulated power supply, an embedded computer, control electronics, actuators, and sensors. Each sub-system will be discussed, and a block diagram of the overall system is shown in Figure 3-1.

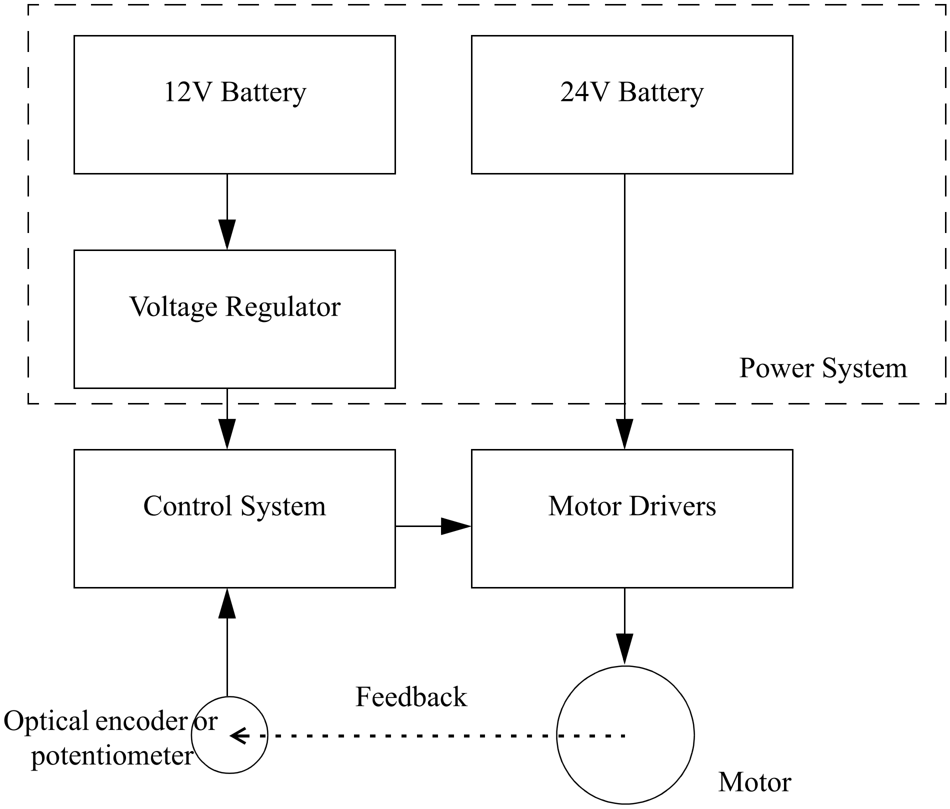
12V Battery
24V Battery
Voltage Regulator
Power System
Control System
Motor Drivers
Feedback
Optical encoder or potentiometer
Motor

Figure 3-1: Block diagram of *Pneuman's* electronics and control systems.

3.2 Power System

Sealed lead-acid batteries were chosen due to their high capacity and low cost. Two 12V, 12Ah batteries are arranged in parallel for 12V@24Ah and two are arranged in series for 24V@12Ah. These four batteries provide *Pneuman* with enough power to operate autonomously for approximately 30 minutes. The 12V system supplies power to the computer voltage regulator and the 24V system powers all of the actuators. See Figure 3-2.

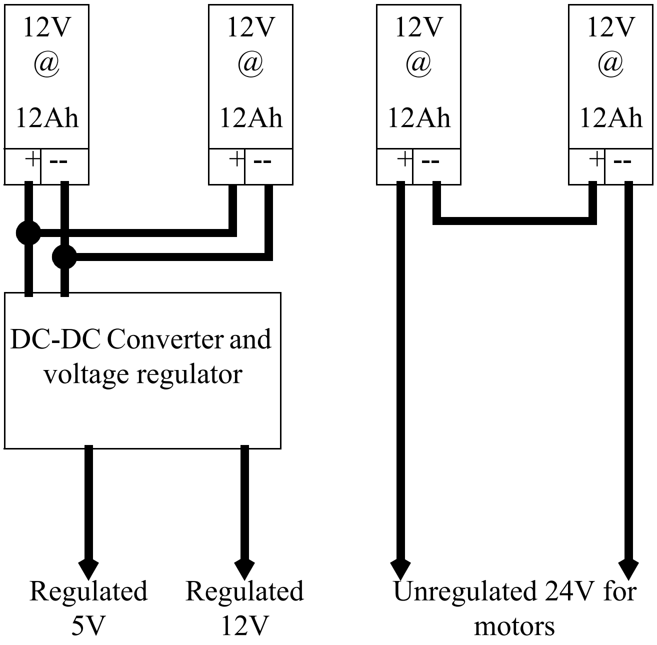
12V
@
12Ah
+
--
12V
@
12Ah
+
--
12V
@
12Ah
+
--
12V
@
12Ah
+
--
DC-DC Converter and voltage regulator
Regulated 5V
Regulated 12V
Unregulated 24V for motors

Figure 3-2: *Pneuman's* battery and power system.

3.3 Computer System

3.3.1 Hardware

Pneuman's computer is a JUMPtec Intel Pentium with a 166 MHz internal clock and 32 kB of write-back-cache. It has 128 MB of SDRAM, an 18 GB hard disk drive, a 100 BaseT ethernet connection, two serial ports, one parallel port, a floppy driver interface, a real time clock, and 128 kB FLASH BIOS. The computer is in a pc/104 form factor, making it ideal for an embedded control system.

The pc/104 bus allows for easy expansion. A voice synthesizer module from RC Systems, Inc. connects to the pc/104 bus and provides *Pneuman* with the ability to speak an infinite number of words. Additionally, wireless communication is possible with the use of a pc/104 to PCMCIA wireless network card adapter. Other modules using the pc/104 bus include the PWM module and the PID module. These two modules form the main components of the digital control systems on *Pneuman*.

3.3.2 Software

The operating system is Mandrake Linux 8.1. Software was developed in the *C* programming language. The code is modular; each module is a separate process that communicates via a shared memory space. The main executable is a process manager that initializes memory space for the other processes and executes the requested modules. The current modules display the text user interface, generate the timer signals, and execute the control algorithms. See Figure 3-3.

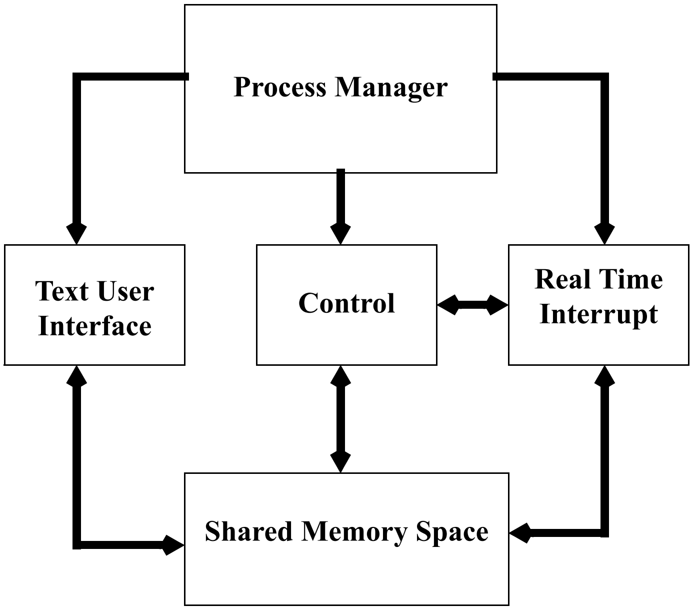

Figure 3-3: Software structure.

The results from the processes are then sent to the other modules via a shared memory space. The movement control module keeps precise records of the current and desired states of all the actuators. This data is used to determine what control output is necessary to move to a desired position. The text-based user interface module allows the user of the system to change the parameters for *Pneuman*.

3.4 Pulse Width Modulation (PWM) System

All of the actuators on *Pneuman* are brushed direct current (DC) motors. Their torque is controlled by pulse width modulating their current. The control signals are generated by custom pc/104 cards. Each card has three main systems, including PWM components, digital input/output (IO) components, and an analog-to-digital converter. The overall goal is to provide a complete proportional, integral, and derivative (PID) controller for each motor, implemented in software. This will be possible by using the analog inputs for angle position sensors, and controlling the motors via a motor driver board with PWM and direction signals.

The first system is responsible for generating PWM using three standard 8254 programmable timers. Each timer chip contains three individual timers, for a total of nine timers on each pc/104 board. Each timer has a count register and an output pin associated with it. When the count register reads zero, an event on the corresponding timer pin may occur. An event may involve the output going high, low, changing from its current state, or nothing at all. One of the timers is set to operate as a real-time interrupt (RTI) providing a signal that corresponds to the period of the PWM signals. Note that all eight of the PWM signals generated must have the same period. This RTI signal is connected to the trigger inputs of all the other timers. Furthermore, the remaining eight timers are operating in “one-shot” mode. This means that once the trigger is asserted, the outputs of these timers are asserted until their corresponding timers count down to zero, thereby de-asserting the output. Additionally, the values in the count registers may be loaded with different values via the pc/104 bus, thereby changing the time that the outputs remain high. Thus, this may be used in combination with the RTI as mentioned above for hardware PWM [27]. See Figure 3-4.

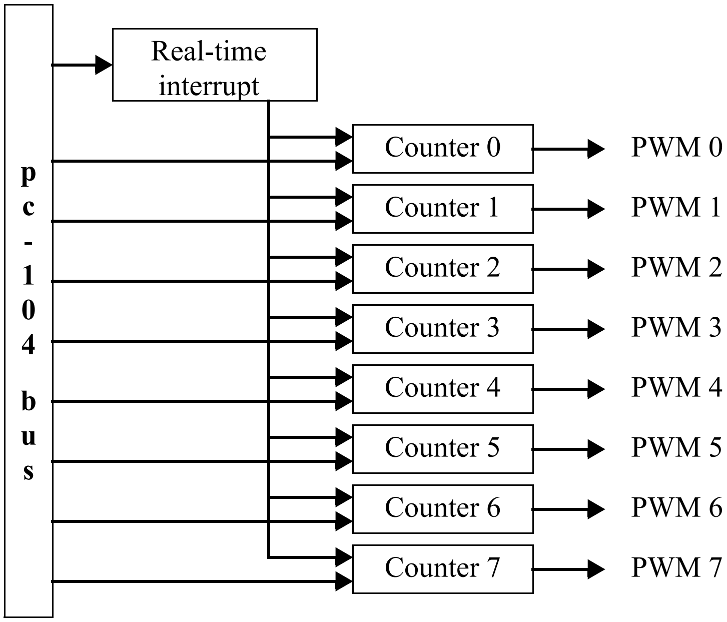
Real-time interrupt
p c - 1 0 4 b u s
Counter 0
Counter 1
Counter 2
Counter 3
Counter 4
Counter 5
Counter 6
Counter 7
PWM 0
PWM 1
PWM 2
PWM 3
PWM 4
PWM 5
PWM 6
PWM 7

Figure 3-4: Pulse width modulation system.

The next system provides eight digital input/output connections (IO's) for the direction control of each motor, eight outputs to control the analog to digital converter, and eight inputs to read the analog values. This system uses a standard Intel 8255 parallel peripheral interface (PPI) IC. The final component of the board, the analog-to-digital conversion system, uses an Analog Devices ADC0808 IC. This particular IC provides eight input channels as well as eight bits of resolution for each channel [27]. See figure 3-5. An image of the pc/104 card is shown in Figure 3-6.

3.5 Hardware-Implemented Control System

The above mentioned PWM boards are ideal for a closed loop position control system utilizing a potentiometer for feedback. However, the drive wheels use an incremental quadrature optical encoder for feedback. The encoders allow 360° of rotation, as required for a drive wheel, and the incremental count permits significant wheel travel before the counter can overflow. A different system was required to control the velocity and position of the drive wheels because incremental encoders are used. Therefore, custom pc/104 cards were designed to interface to the encoders and control the corresponding drive motors.

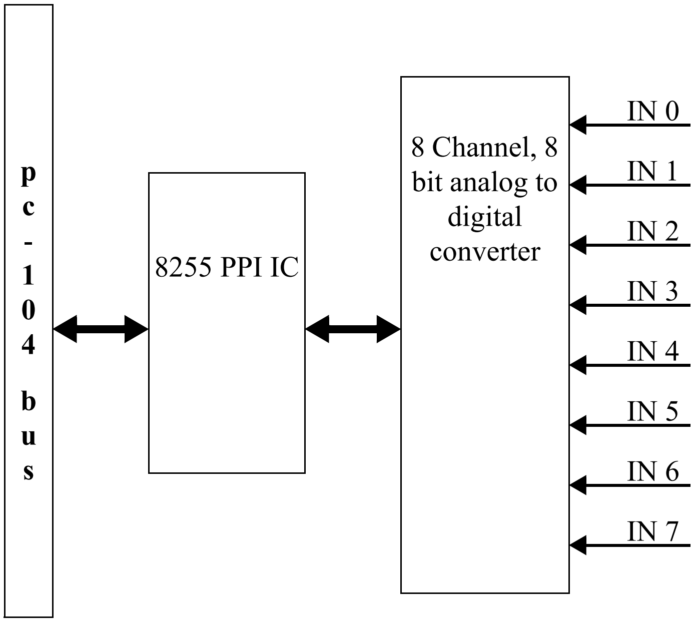
pc-104 bus
8255 PPI IC
8 Channel, 8 bit analog to digital converter
IN 0
IN 1
IN 2
IN 3
IN 4
IN 5
IN 6
IN 7

Figure 3-5: Analog to digital conversion system.

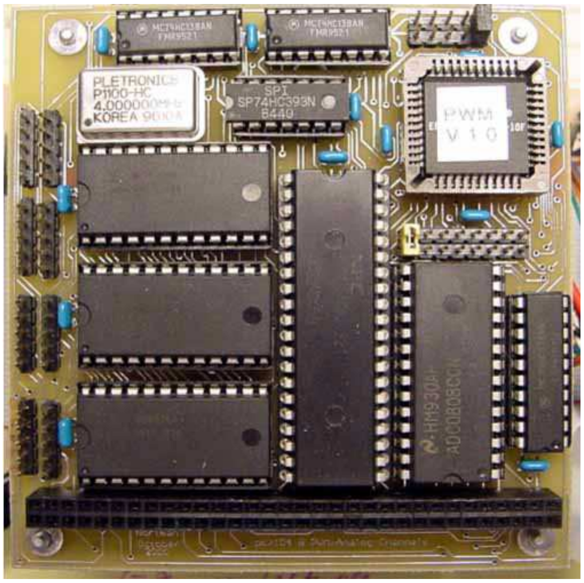

Figure 3-6: Image of the PWM and A to D pc/104 card.

The boards have four National Semiconductor LM629 motion control IC's. The embedded computer interfaces to these IC's via the pc/104 bus. They are dedicated motion control processors that use a quadrature incremental position feedback signal. The optical encoders mounted directly to each drive wheel provide these signals. There are four PWM outputs (each with eight bit resolution), for directly driving an H-bridge motor driver. Each IC may operate in position and velocity mode or velocity only mode. Position and velocity mode will be useful for doing navigation through dead reckoning. Velocity mode will insure that the wheels are all operating at the appropriate speeds even if distance information is not needed [28]. See Figure 3-7.

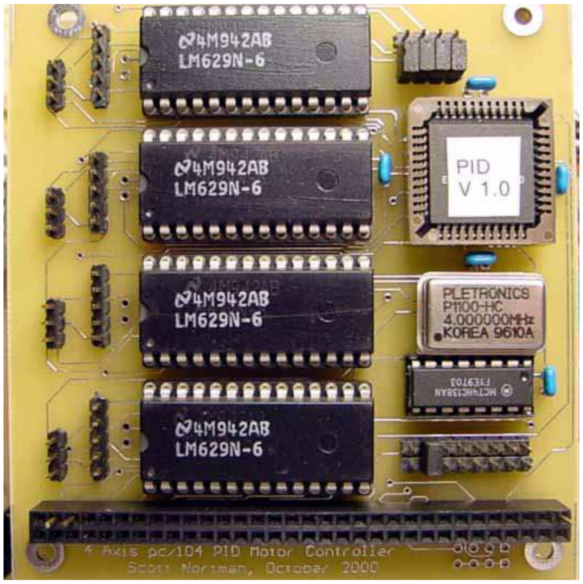
4M942AB
LM629N-6
4M942AB
LM629N-6
4M942AB
LM629N-6
4M942AB
LM629N-6
PID
V 1.0
PLETRONICS
P1100-HC
4.000000MHz
KOREA 9610A
4 Axis pc/104 PID Motor Controller
Scott Norman, October 2000

Figure 3-7: Image of LM629 pc/104 card.

3.6 Solid State Motor Drivers

The PWM and PID systems generate the digital control signals for the motors. The control signals are connected to solid state *H-Bridge* motor drivers. The motor drivers act as amplifiers, allowing the logic level signals control the high current from the batteries. The motor drivers contain four metal oxide semiconductor field effect transistors (MOSFETs) arranged in an H configuration. This allows current to flow in both directions to the motor, controlling the direction of rotation. The switches can turn the current on and of rapidly, controlling the speed of the motors [26]. The details of this control method are discussed in Chapter 4. See Figure 3-8 for a block diagram, and Figure 3-9 for an image of the circuit board.

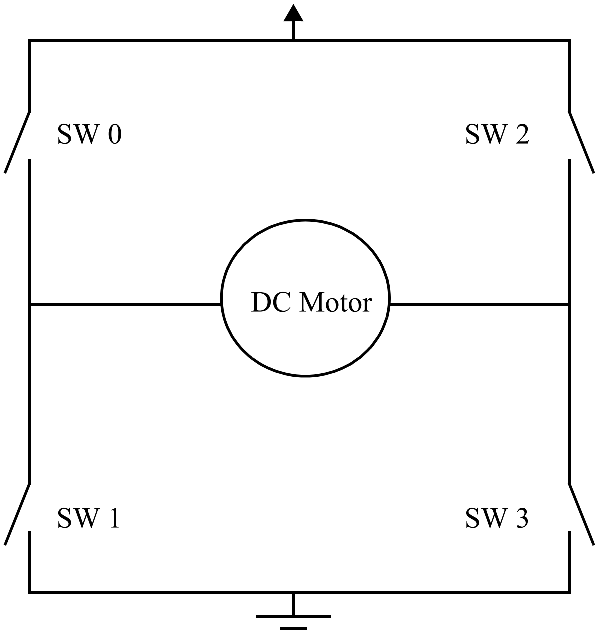
SW 0
SW 2
DC Motor
SW 1
SW 3

Figure 3-8: Block diagram of the H-bridge motor driver.

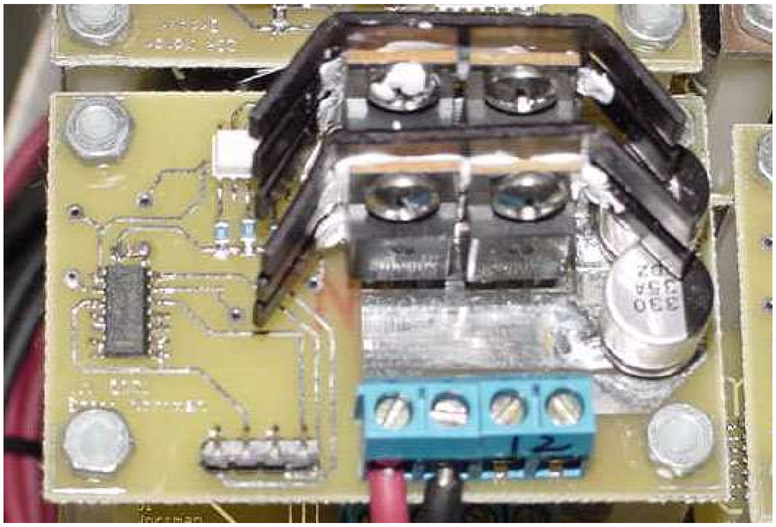

Figure 3-9: Solid state H-bridge motor driver.

CHAPTER 4
CONTROL THEORY

4.1 Overview

Pneuman's mechanical structure has 25 degrees of freedom (DOF). Each DOF is actuated by a direct current (DC) motor and has a sensor for feedback. The embedded computer analyzes the information from the sensor and controls the corresponding DC motor to achieve the desired output. Each DOF, with its own DC motor and sensor, constitutes a complete closed loop control system. There are two different types of sensors used on *Pneuman*; potentiometers provide absolute joint position for 19 of the 25 DOF and incremental optical encoders are used on the drive wheels and stereo head. The details regarding the use of each sensor will be discussed in the following sections.

Although a control system provides a way to achieve a desired output, the methods used to determine what the desired output should be are also considered. For example, if a particular joint is positioned at 0 degrees and the desired position is 90 degrees, how should the joint move from the initial to the final position? Do you simply command the controller to position the joint at 90 degrees as fast as possible? Will that cause too much mechanical strain on the joint? What if you wanted it to move “smoothly” over a period of 5 seconds? These issues, commonly known as *joint trajectory generation,* will also be discussed in detail.

4.2 Control of Direct Current (DC) Motors

Essentially, a DC motor consists of a stator, a rotor, and a commutator. The stator is the housing of the motor and contains magnets, bearings, etc.. The rotor is the rotating part of the motor and contains a coil of wire through which current flows. The coil of wire in the rotor connects to the commutator and receives current via brushes. The commutator insures that the current flows in the proper direction while the rotor turns [26].

In understanding this topic, it is important to have an understanding of the operation and mathematical model of a DC motor. When current flows through the coil of wire in the rotor, a torque is created that causes the rotor to spin. The relationship between the motor output torque and the current is given by

$${}_m = k_m i_a \tag{4-1}$$

where ${}_m$ is the output torque, k_m is the torque constant, and i_a is the rotor coil current. Consequently, the amount of torque generated is proportional to the current flowing through the wire. However, there is a limit to the amount of torque a given motor can produce. The coil of wire in the rotor is an inductor, and the voltage across the inductor is

$$v = L\frac{di}{dt} \tag{4-2}$$

where v is the voltage across the coil, L is the inductance of the coil, and $\frac{di}{dt}$ is the changing current across the inductor. This coil-induced voltage opposes the voltage that is applied to the motor, causing a *decrease* in current through the rotor. This is called the *back-emf voltage* and the negative feedback eventually causes the motor to settle at a steady state point of operation [26].

Changing the voltage across the motor terminals will vary the current flowing through the coil thereby changing the torque produced by the motor. However, this technique is not used to control *Pneuman's* motors. Instead, a constant voltage is pulsed through the motor coil. This pulsing, or pulse width modulation (PWM), changes the *average* current through the motor over time. The average current is proportional to the *duty cycle* of the PWM signal. The *duty cycle* is determined by

$$\%\ \text{duty cycle} = \frac{\text{high time}}{\text{period}}\ 100\%\,. \tag{4-3}$$

See Figure 4-1 [26].

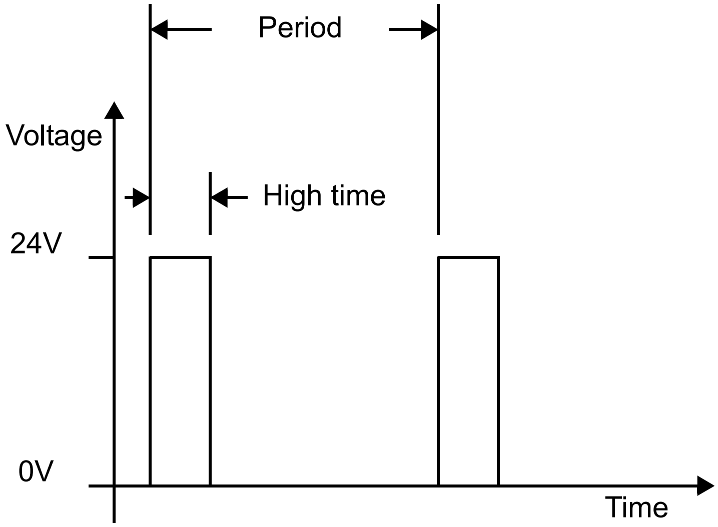

Figure 4-1: Pulse width modulation

4.3 Control System Implementation

4.3.1 Analog Feedback Control

Nineteen of *Pneuman's* joints use analog potentiometers for feedback. They operate as absolute position encoders, providing a voltage reference indicating the joint angle. This voltage signal is fed into an analog to digital converter, providing eight-bits of resolution over the potentiometer's operational range of 300 degrees. Therefore each bit corresponds to 1.17 degrees of movement, which is acceptable for *Pneuman's* designated purpose as an experimental research platform. See Figure 4-2.

All of the joints utilizing a potentiometer use a discrete approximation of the proportional, derivative, and integral (PID) control law, with gravity compensation (except for the steering mechanisms), implemented in software. This robust control law was selected due to its simplicity and good performance. The discrete PID controller is implemented with equation 4-4:

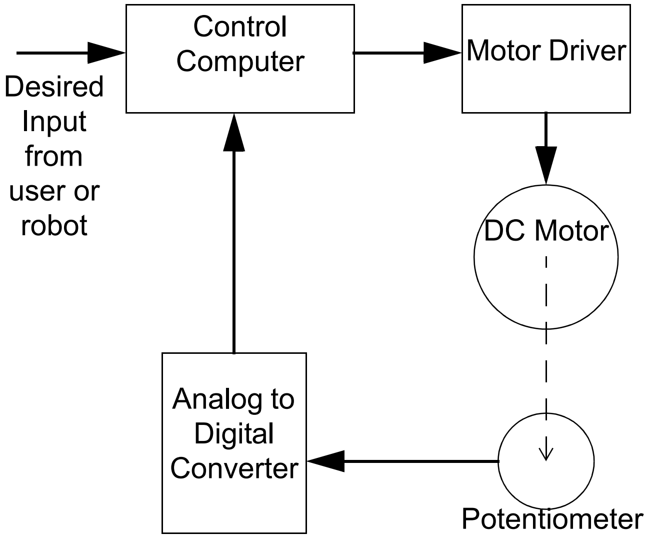

Figure 4-2: Block diagram of analog control system.

$$n \; = k_P \;\; e \;\; n \;\; + k_I \quad {}^{N}_{n\,=\,0} \;\; e \;\; n \;\; + k_D \;\; e \;\; n \;\; - e \;\; n - 1 \quad , \tag{4-4}$$

where n is the motor control signal output, updated at the sampling time n, k_P is the proportional gain, k_I is the integral gain, k_D is the derivative gain, and $e(n)$ is the position error at the sample time n. All of the joints have the same sampling rate of 100 Hz, and all of the gains are individually tuned for maximum performance [28], [29].

The potentiometers used as joint angle sensors may have nonlinear characteristics. For example, the potentiometer may physically rotate 90 degrees, but due to the nonlinear characteristics the analog value does not indicate a change of 90 degrees. See Figure 4-3. Therefore, all of the joints must be calibrated to get the most accurate measurements possible. Ideally, a large data set collected over the complete range of motion should be collected and used for an accurate calibration. However, collecting data over the complete range of motion for each DOF is not feasible due to difficulties in obtaining accurate position measurements without

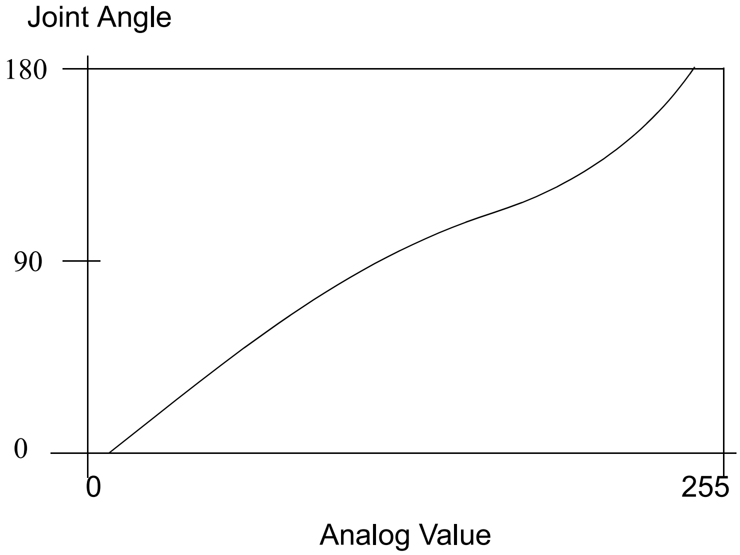

Figure 4-3: Output of uncalibrated potentiometer

sophisticated tools. For this reason, three data points are collected and used to calibrate each joint.

The three data points form two lines; the slopes and y-axis intercepts of each line are the calibration parameters for each DOF. The slopes are determined from the following equations:

$$\text{slope}_A = \frac{\text{Joint Position}}{\text{Analog Value}} = \frac{\text{Position 1} - \text{Position 0}}{\text{Analog 1} - \text{Analog 0}} \qquad (4\text{-}5)$$

$$\text{slope}_B = \frac{\text{Joint Position}}{\text{Analog Value}} = \frac{\text{Position 2} - \text{Position 1}}{\text{Analog 2} - \text{Analog 1}} \qquad (4\text{-}6)$$

and the intercepts from

$$\text{Intercept A} = \text{Position 1} - \ \text{slope}_A \ \ \text{Analog 1} \qquad (4\text{-}7)$$

$$\text{Intercept B} = \text{Position 1} - \ \text{slope}_B \ \ \text{Analog 1} \qquad (4\text{-}8)$$

For example, each drive wheel is calibrated at -90, 0, and +90. The corresponding analog values are recorded and used to calibrate the joint. The calculated calibration lines are then used to interpolate joint position between the calibration points. See Figure 4-4.

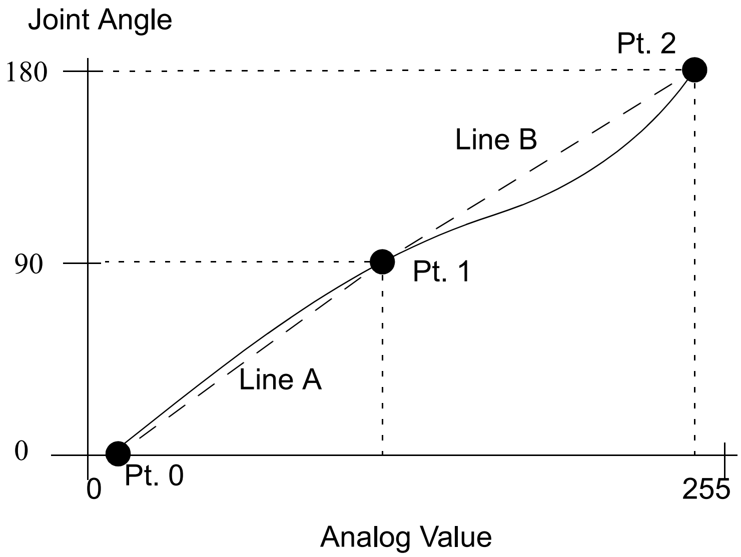

Figure 4-4: Calibrated potentiometer plot

4.3.2 Digital Feedback Control

Pneuman's drive wheels and stereo head actuators each use incremental optical encoders for feedback. These non-contact sensors permit a full 360 degrees of rotation, a requirement for the drive wheels. The wheel encoders have a resolution of 0.18 degrees, allowing for precision distance measurement. The stereo head convergence optical encoders have a resolution of 0.036 degrees, which is needed for precision stereo vision. Each of the encoders connects to a National Semiconductor LM629 motion control integrated circuit (IC). This specialty-purpose controller interfaces directly to an optical encoder and outputs a signed-magnitude PWM signal for motor control. See Figure 4-5.

The LM629 is a specialty purpose micro controller which interfaces directly to a quadrature optical encoder for feedback. *Pneuman's* main computer issues commands to the LM629 via the pc/104 bus, and the IC generates the desired motion trajectory. The PID filter is given by equation 4-9:

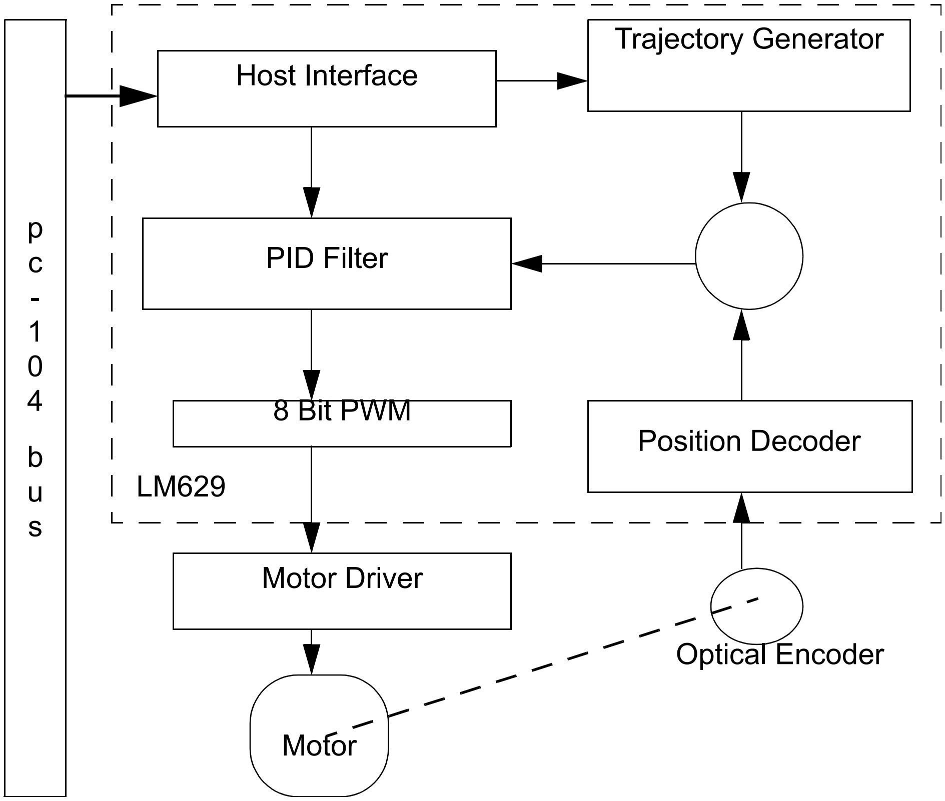
pc-104 bus
Host Interface
Trajectory Generator
PID Filter
8 Bit PWM
Position Decoder
LM629
Motor Driver
Optical Encoder
Motor

Figure 4-5: LM629 PID controller block diagram.

$$n = k_P \;\; e \;\; n \; + k_I \overset{N}{\underset{n=0}{}} e \;\; n \; + k_D \; e \;\; n' \; - e \;\; n' - 1 \qquad (4\text{-}9)$$

where n is the motor control signal output, updated at the sampling time n, $e(n)$ is the position error at the sample time n, n' indicates the derivative sampling rate, k_P is the proportional gain, k_I is the integral gain, and k_D is the derivative gain [28].

The proportional term contributes a restoring force proportional to the positional error. The integral term provides a restoring force that is summed over time, insuring that the static error is zero. Therefore, even if there is a constant load on the motor, zero error will still be achieved. The final derivative term provides a damping force, which is proportional to the rate of error change [28].

4.4 Joint Trajectory Generation

4.4.1 Software Trajectory Generation

The overall desired motions of a manipulator may be considered a multidimensional trajectory, which is a history of position, velocity and acceleration versus time. While a qualitative description of a trajectory appears trivial (i.e., make the end-effector go from point A to point B), a quantitative description is more difficult. Questions such as, “How fast should the manipulator move?” and, “What if there is an obstacle in the way?” need to be addressed. Even though a quantitative description is not trivial to compute, an end user of a robotic system should not have to deal with all details of the desired motions. Instead, a goal position and orientation may be given and the control system calculates the best way to get there.

There are a number of ways to move a robot from point A to point B, but they all share a common attribute; they allow the robot to move “smoothly.” A motion may be considered smooth if it is continuous and differentiable. This type of motion decreases wear on the mechanics, reduces vibrations, and generally improves the performance of a manipulator [29].

Calculating a smooth trajectory requires that some constraints be placed on the paths between the points along a trajectory. These constraints guarantee a smooth path will be executed, and they must meet the following conditions:

$$0 = {}_0, \tag{4-10}$$

$$t_f = {}_f, \tag{4-11}$$

which are the initial and final joint position values at the initial and final times, respectively. Two other constraints are given by:

$$\dot{}\ 0 = 0, \tag{4-12}$$

$$\dot{}\; t_f = 0, \tag{4-13}$$

indicating that the initial and final velocities are zero.

These four constraints necessitate a function with four coefficients, a cubic polynomial. A cubic polynomial has the following form:

$$t = a_0 + a_1 t + a_2 t^2 + a_3 t^3, \tag{4-14}$$

with velocity and acceleration given by:

$$\dot{}\; t = a_1 + 2a_2 t + 3a_3 t^2, \tag{4-15}$$

$$\ddot{}\; t = 2a_2 + 6a_3 t. \tag{4-16}$$

By taking the previous constraints and combing them with the cubic and the derivatives we get a system of four equations and four unknowns; therefore we can solve for the cubic polynomial coefficients:

$$a_0 = {}_0, \tag{4-17}$$

$$a_1 = 0, \tag{4-18}$$

$$a_2 = \frac{3}{t_f^2}\; {}_f - {}_0 , \tag{4-19}$$

$$a_3 = -\frac{2}{t_f^3}\; {}_f - {}_0 \tag{4-20}$$

where ${}_0$ is the initial position, ${}_f$ is the final position, and t_f is the amount of time allotted to complete the trajectory [29].

The trajectories of *Pneuman's* drive wheels are determined using this method. This simple trajectory generation scheme was chosen because the steering assembly does not require additional constraints on the velocities and accelerations. The amount of time required to execute any given trajectory is determined by taking the ratio of the desired movement over the overall range of motion and multiplying by the time allowed for the full range of motion:

$$t_{allotted} = \frac{{}_{given}}{{}_{total}} \; t_{total} \tag{4-21}$$

with ${}_{total}$ and t_{total} varying for the different joints. The steering joints all use 180 degrees and 3 seconds, respectively.

For example, a steering trajectory executed with a starting position of -45 degrees and an ending position of 30 degrees will have the following parameters:

$$t_{allotted} = \frac{{}_{given}}{{}_{total}} \; t_{total} = \frac{75}{180} \; 3s = 1.25s \tag{4-22}$$

$$a_0 = {}_0 = -45 \tag{4-23}$$

$$a_1 = 0 \tag{4-24}$$

$$a_2 = \frac{3}{t_f^2} \; {}_f - {}_0 = 144 \tag{4-25}$$

$$a_3 = -\frac{2}{t_f^3} \; {}_f - {}_0 = -76.8 \tag{4-26}$$

and the cubic is

$$t = -45t + 144t^2 - 76.8t^3 \tag{4-27}$$

and the plot of the above trajectory is shown in Figure 4-6.

The previously described method may be applied if the starting and ending velocities are zero. However, if intermediate *via points* are needed where the velocities are not zero, the cubic coefficients are determined by:

$$a_0 = \theta_0 , \tag{4-28}$$

$$a_1 = \dot{\theta}_0 , \tag{4-29}$$

$$a_2 = \frac{3}{t_f^2}\left(\theta_f - \theta_0\right) - \frac{2}{t_f}\dot{\theta}_0 - \frac{1}{t_f}\dot{\theta}_f , \tag{4-30}$$

$$a_3 = -\frac{2}{t_f^3}\left(\theta_f - \theta_0\right) + \frac{1}{t_f^2}\left(\dot{\theta}_f + \dot{\theta}_0\right) , \tag{4-31}$$

where θ_0 is the starting position, $\dot{\theta}_0$ is the starting velocity, θ_f is the final position, and $\dot{\theta}_f$ is the final velocity of the segment. Although the steering and drive assemblies do not use this technique, the rest of *Pneuman's* joints benefit from the ability to use via points. See Figure 4-7 for a cubic trajectory with via points; the first segment from -45 degrees to 30 degrees occurs in 1.5 seconds with a via point velocity of 20 degrees/second, and the second segment from 30 to 75 degrees occurs in 3 seconds with and ending velocity of 0 degrees/second [29].

4.4.2 Hardware Trajectory Generation

The LM629 motion control IC does not use cubic trajectory generation. Instead, an alternate generation scheme with a trapezoidal profile is used. In positional control mode, the profile is generated by specifying the desired values of acceleration, maximum allowable velocity, and desired final position. The motion controller uses this information to affect the move by accelerating continuously until the maximum velocity is reached or deceleration must begin to stop at the desired final position. During the move, the values of maximum velocity and desired stopping position may be changed to alter the trajectory [28].

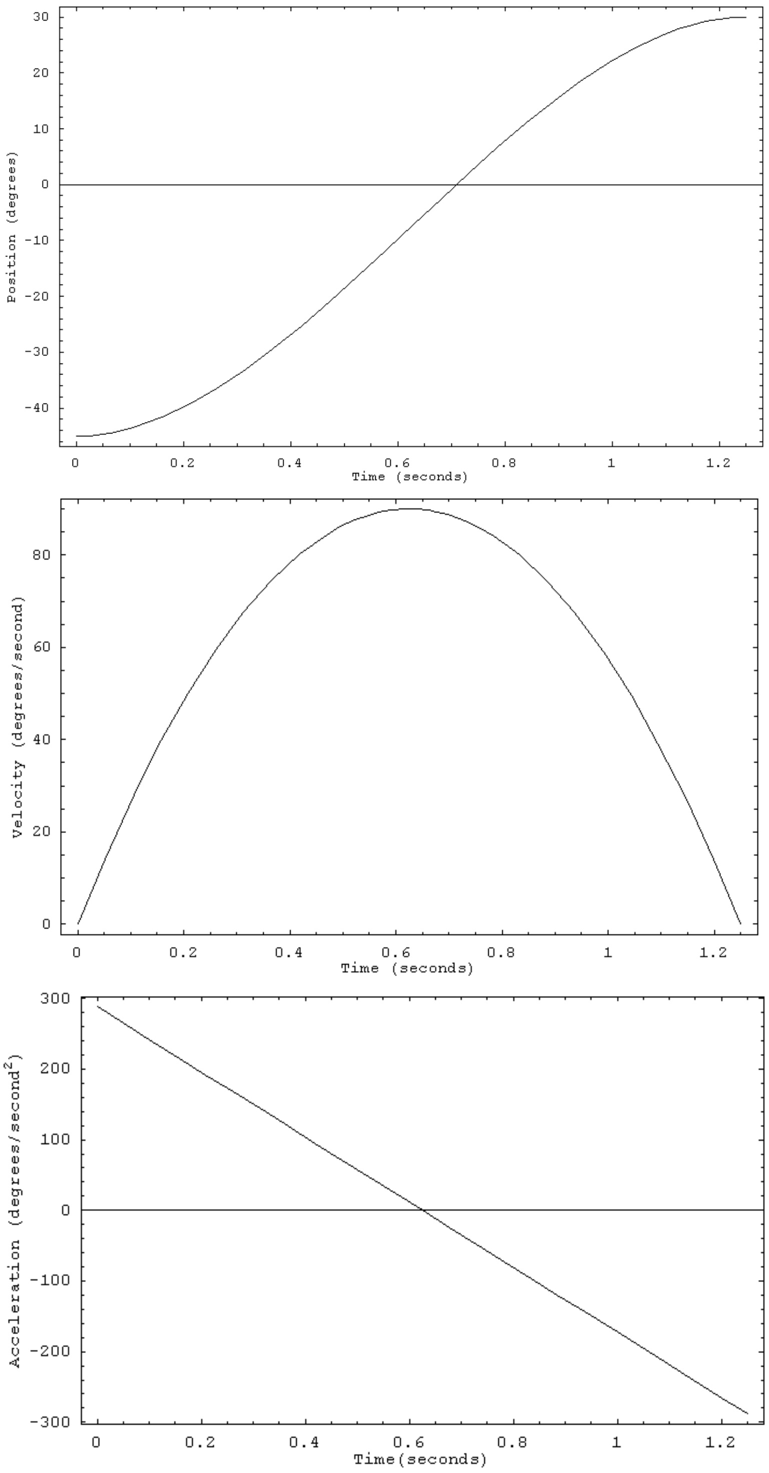

Figure 4-6: Plot of desired cubic trajectory from -45 degrees to 30 degrees in 1.25 seconds without via points.

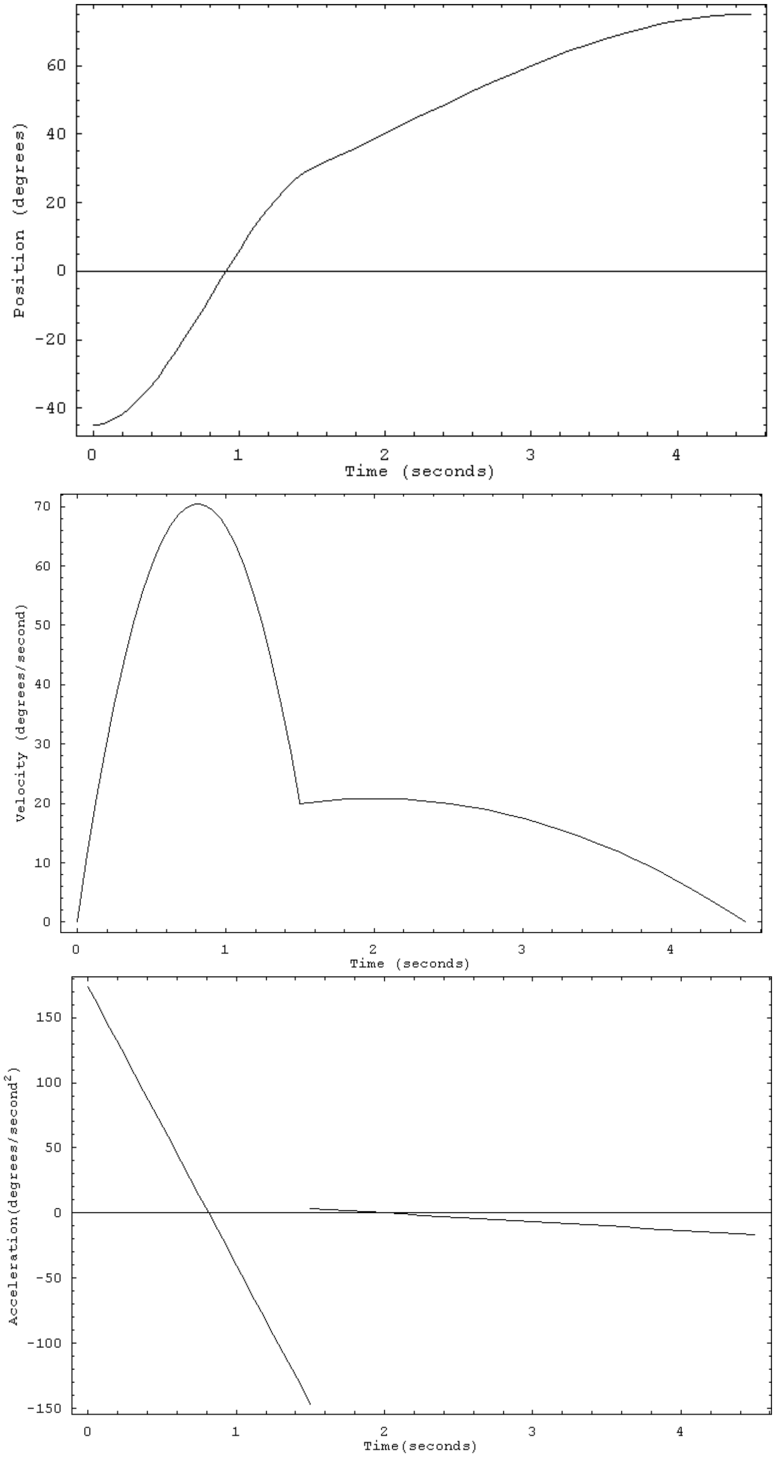

Figure 4-7: Trajectory with *via points*.

In velocity-only control mode, the values of acceleration and maximum velocity are used to generate the trajectory. The LM629 causes the motor to accelerate to the specified velocity until the maximum allowable velocity is reached, and maintains this velocity until commanded to stop. Again, the deceleration rate is equal to the acceleration rate. See Figure 4-8 for typical trajectories [28].

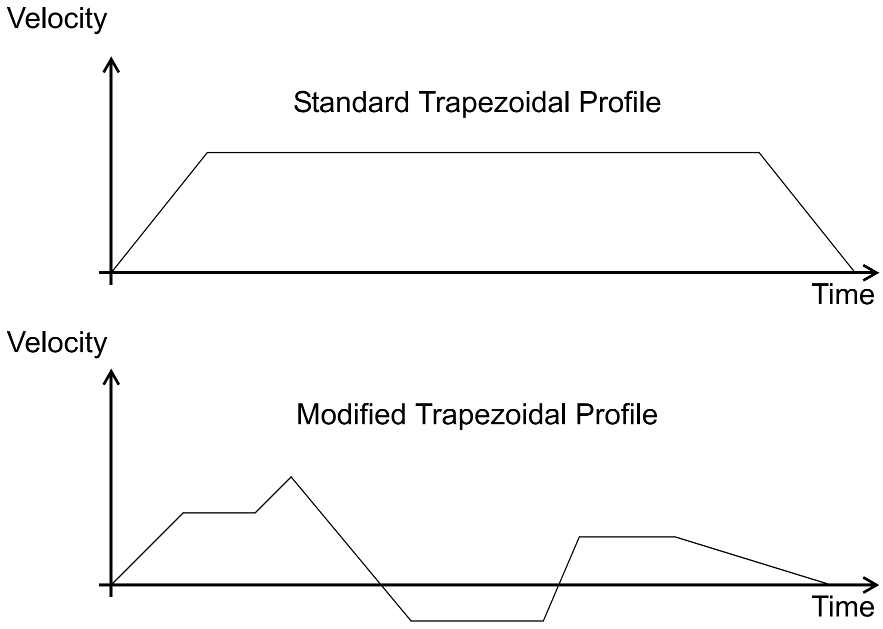
Velocity
Standard Trapezoidal Profile
Time
Velocity
Modified Trapezoidal Profile
Time

Figure 4-8: Typical LM629 Motion Trajectories

CHAPTER 5
USER INTERFACE

Eventually, *Pneuman* will operate autonomously, but this is not the case during development. The user requires control over all of *Pneuman's* parameters during development to insure that the robot functions properly. Therefore, a text user interface is currently under development. This interface allows all of *Pneuman's* joint parameters to be calibrated, adjusted, and controlled. The initial startup screen allows the user to select a parameters menu or a control menu. See Figure 5-1.

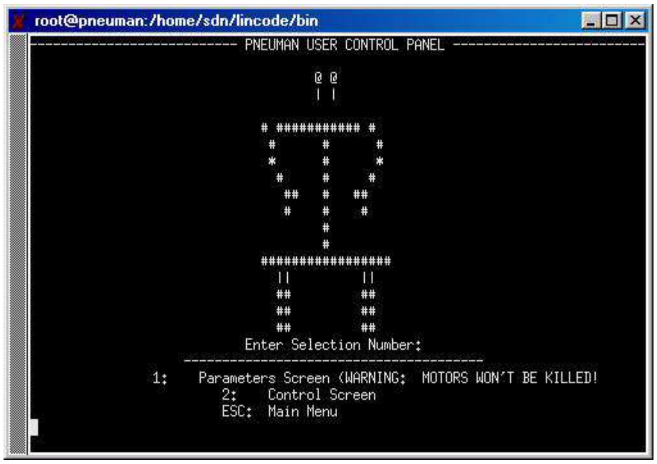

```
--------------------------- PNEUMAN USER CONTROL PANEL -------------------------

                                      @ @
                                      | |

                               # ########### #
                                #      #      #
                                *      #      *
                                 #     #     #
                                  ##   #   ##
                                  #    #    #
                                       #
                                       #
                               #################
                                 ||         ||
                                 ##         ##
                                 ##         ##
                                 ##         ##
                            Enter Selection Number:
                    ----------------------------------------
                1:    Parameters Screen (WARNING:  MOTORS WON'T BE KILLED!
                         2:    Control Screen
                         ESC:  Main Menu
```

Figure 5-1: Initial Startup Screen of User Interface

The parameters menu shows all of the attributes of *Pneuman's* DOF. The control loop parameters are *actual position, desired position, minimum position, maximum position, default position, kp, ki, kd,* and *duty cycle*. Note that the *duty cycle* can not be displayed for the LM629 control loops because it is implemented in hardware. See Figure 5-2. All of the user adjusted attributes can be set from this menu. Each option may be selected by pressing the appropriate key, identified as a capital letter on the menu bar at the top of the program window.

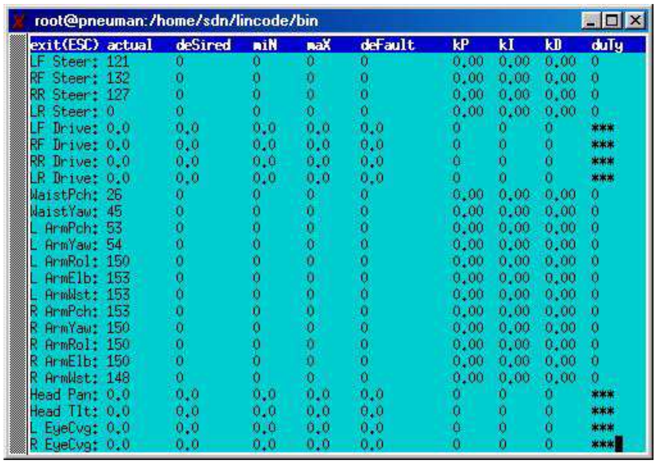

```
exit(ESC) actual deSired  miN    maX    deFault   kP    kI    kD    duTy
LF Steer: 121    0        0      0      0         0.00  0.00  0.00  0
RF Steer: 132    0        0      0      0         0.00  0.00  0.00  0
RR Steer: 127    0        0      0      0         0.00  0.00  0.00  0
LR Steer: 0      0        0      0      0         0.00  0.00  0.00  0
LF Drive: 0.0    0.0      0.0    0.0    0.0       0     0     0     ***
RF Drive: 0.0    0.0      0.0    0.0    0.0       0     0     0     ***
RR Drive: 0.0    0.0      0.0    0.0    0.0       0     0     0     ***
LR Drive: 0.0    0.0      0.0    0.0    0.0       0     0     0     ***
WaistPch: 26     0        0      0      0         0.00  0.00  0.00  0
WaistYaw: 45     0        0      0      0         0.00  0.00  0.00  0
L ArmPch: 53     0        0      0      0         0.00  0.00  0.00  0
L ArmYaw: 54     0        0      0      0         0.00  0.00  0.00  0
L ArmRol: 150    0        0      0      0         0.00  0.00  0.00  0
L ArmElb: 153    0        0      0      0         0.00  0.00  0.00  0
L ArmWst: 153    0        0      0      0         0.00  0.00  0.00  0
R ArmPch: 153    0        0      0      0         0.00  0.00  0.00  0
R ArmYaw: 150    0        0      0      0         0.00  0.00  0.00  0
R ArmRol: 150    0        0      0      0         0.00  0.00  0.00  0
R ArmElb: 150    0        0      0      0         0.00  0.00  0.00  0
R ArmWst: 148    0        0      0      0         0.00  0.00  0.00  0
Head Pan: 0.0    0.0      0.0    0.0    0.0       0     0     0     ***
Head Tlt: 0.0    0.0      0.0    0.0    0.0       0     0     0     ***
L EyeCvg: 0.0    0.0      0.0    0.0    0.0       0     0     0     ***
R EyeCvg: 0.0    0.0      0.0    0.0    0.0       0     0     0     ***
```

Figure 5-2: Parameters menu.

For example, the "S" key is pressed to set the desired position of a joint. After the initial key press, a sub-window appears allowing the user to select the particular joint. Once the joint is selected, a window appears asking for a new desired position. See Figure 5-3.

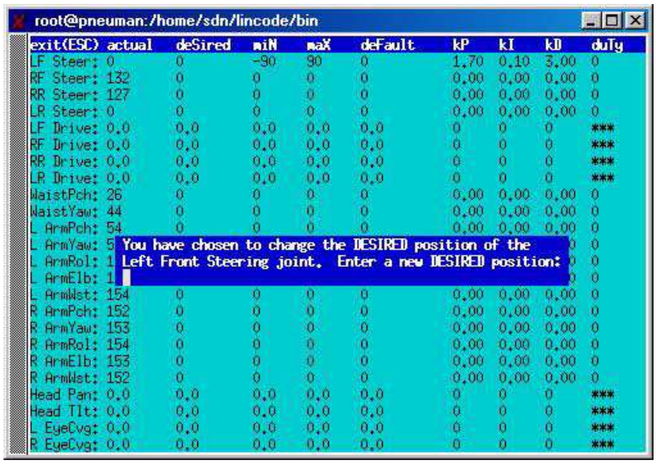

```
exit(ESC) actual deSired  miN    maX    deFault   kP    kI    kD    duTy
LF Steer: 0      0        -90    90     0         1.70  0.10  3.00  0
RF Steer: 132    0        0      0      0         0.00  0.00  0.00  0
RR Steer: 127    0        0      0      0         0.00  0.00  0.00  0
LR Steer: 0      0        0      0      0         0.00  0.00  0.00  0
LF Drive: 0.0    0.0      0.0    0.0    0.0       0     0     0     ***
RF Drive: 0.0    0.0      0.0    0.0    0.0       0     0     0     ***
RR Drive: 0.0    0.0      0.0    0.0    0.0       0     0     0     ***
LR Drive: 0.0    0.0      0.0    0.0    0.0       0     0     0     ***
WaistPch: 26     0        0      0      0         0.00  0.00  0.00  0
WaistYaw: 44     0        0      0      0         0.00  0.00  0.00  0
L ArmPch: 54     0        0      0      0         0.00  0.00  0.00  0
L ArmYaw: 5 You have chosen to change the DESIRED position of the  0  0
L ArmRol: 1 Left Front Steering joint.  Enter a new DESIRED position:  0  0
L ArmElb: 1                                                        0  0
L ArmWst: 154    0        0      0      0         0.00  0.00  0.00  0
R ArmPch: 152    0        0      0      0         0.00  0.00  0.00  0
R ArmYaw: 153    0        0      0      0         0.00  0.00  0.00  0
R ArmRol: 154    0        0      0      0         0.00  0.00  0.00  0
R ArmElb: 153    0        0      0      0         0.00  0.00  0.00  0
R ArmWst: 152    0        0      0      0         0.00  0.00  0.00  0
Head Pan: 0.0    0.0      0.0    0.0    0.0       0     0     0     ***
Head Tlt: 0.0    0.0      0.0    0.0    0.0       0     0     0     ***
L EyeCvg: 0.0    0.0      0.0    0.0    0.0       0     0     0     ***
R EyeCvg: 0.0    0.0      0.0    0.0    0.0       0     0     0     ***
```

Figure 5-3: Setting the desired position of the left front steering joint.

After a desired value is entered, the joint moves to the desired position. Upon finishing the move, a real time plot of the desired trajectory, actual trajectory, and trajectory error is printed to the screen. See Figure 5-4.

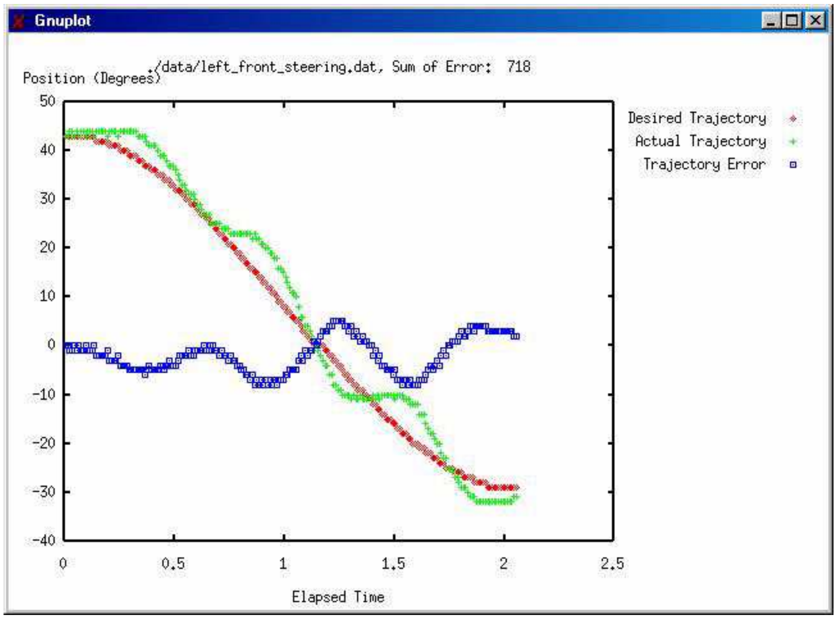

Figure 5-4: Real-time plot of desired, actual, and error trajectory values.

The parameters screen also accesses the calibration utility for the analog sensor joints. The utility allows the user to control the joint with the keyboard. Initially, the user is prompted to position the joint at the position corresponding to -90 degrees and then to press the ENTER key. Next, the joint is positioned at 0 degrees. Finally, the DOF is positioned at +90 degrees. After the three analog values are determined, the calibration slope and intercept values are calculated and saved to a file so the joints do not need to be calibrated every time the robot is used. See Figure 5-5.

There is also a generic control screen that lets the user drive *Pneuman's* base with four keys: faster, slower, left, and right. This is useful if the robot is under remote control. Later improvements will allow a user to control all of *Pneuman's* joints with a single keystroke. See Figure 5-6.

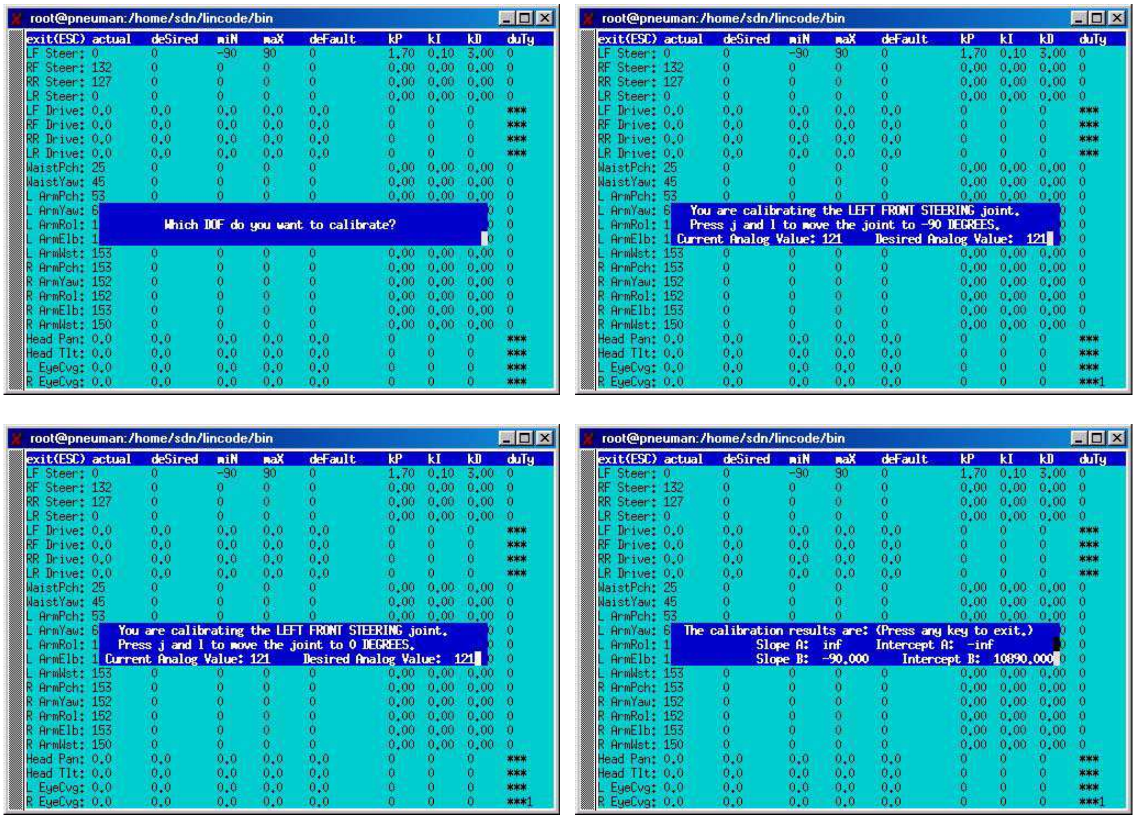
root@pneuman:/home/sdn/lincode/bin
root@pneuman:/home/sdn/lincode/bin
root@pneuman:/home/sdn/lincode/bin
root@pneuman:/home/sdn/lincode/bin

```
exit(ESC) actual  deSired  miN   maX   deFault     kP    kI    kD    duTy
LF Steer: 0       0        -90   90    0           1.70  0.10  3.00  0
RF Steer: 132     0        0     0     0           0.00  0.00  0.00  0
RR Steer: 127     0        0     0     0           0.00  0.00  0.00  0
LR Steer: 0       0        0     0     0           0.00  0.00  0.00  0
LF Drive: 0.0     0.0      0.0   0.0   0.0         0     0     0     ***
RF Drive: 0.0     0.0      0.0   0.0   0.0         0     0     0     ***
RR Drive: 0.0     0.0      0.0   0.0   0.0         0     0     0     ***
LR Drive: 0.0     0.0      0.0   0.0   0.0         0     0     0     ***
WaistPch: 25      0        0     0     0           0.00  0.00  0.00  0
WaistYaw: 45      0        0     0     0           0.00  0.00  0.00  0
L ArmPch: 53      0        0     0     0           0.00  0.00  0.00  0
L ArmYaw: 6                                                    0     0
L ArmRol: 1          Which DOF do you want to calibrate?       0     0
L ArmElb: 1                                                    0     0
L ArmWst: 153     0        0     0     0           0.00  0.00  0.00  0
R ArmPch: 153     0        0     0     0           0.00  0.00  0.00  0
R ArmYaw: 152     0        0     0     0           0.00  0.00  0.00  0
R ArmRol: 152     0        0     0     0           0.00  0.00  0.00  0
R ArmElb: 153     0        0     0     0           0.00  0.00  0.00  0
R ArmWst: 150     0        0     0     0           0.00  0.00  0.00  0
Head Pan: 0.0     0.0      0.0   0.0   0.0         0     0     0     ***
Head Tlt: 0.0     0.0      0.0   0.0   0.0         0     0     0     ***
L EyeCvg: 0.0     0.0      0.0   0.0   0.0         0     0     0     ***
R EyeCvg: 0.0     0.0      0.0   0.0   0.0         0     0     0     ***
```

```
exit(ESC) actual  deSired  miN   maX   deFault     kP    kI    kD    duTy
LF Steer: 0       0        -90   90    0           1.70  0.10  3.00  0
RF Steer: 132     0        0     0     0           0.00  0.00  0.00  0
RR Steer: 127     0        0     0     0           0.00  0.00  0.00  0
LR Steer: 0       0        0     0     0           0.00  0.00  0.00  0
LF Drive: 0.0     0.0      0.0   0.0   0.0         0     0     0     ***
RF Drive: 0.0     0.0      0.0   0.0   0.0         0     0     0     ***
RR Drive: 0.0     0.0      0.0   0.0   0.0         0     0     0     ***
LR Drive: 0.0     0.0      0.0   0.0   0.0         0     0     0     ***
WaistPch: 25      0        0     0     0           0.00  0.00  0.00  0
WaistYaw: 45      0        0     0     0           0.00  0.00  0.00  0
L ArmPch: 53      0        0     0     0           0.00  0.00  0.00  0
L ArmYaw: 6   You are calibrating the LEFT FRONT STEERING joint.   0     0
L ArmRol: 1   Press j and l to move the joint to -90 DEGREES.      0     0
L ArmElb: 1  Current Analog Value: 121    Desired Analog Value:  121   0     0
L ArmWst: 153     0        0     0     0           0.00  0.00  0.00  0
R ArmPch: 153     0        0     0     0           0.00  0.00  0.00  0
R ArmYaw: 152     0        0     0     0           0.00  0.00  0.00  0
R ArmRol: 152     0        0     0     0           0.00  0.00  0.00  0
R ArmElb: 153     0        0     0     0           0.00  0.00  0.00  0
R ArmWst: 150     0        0     0     0           0.00  0.00  0.00  0
Head Pan: 0.0     0.0      0.0   0.0   0.0         0     0     0     ***
Head Tlt: 0.0     0.0      0.0   0.0   0.0         0     0     0     ***
L EyeCvg: 0.0     0.0      0.0   0.0   0.0         0     0     0     ***
R EyeCvg: 0.0     0.0      0.0   0.0   0.0         0     0     0     ***1
```

```
exit(ESC) actual  deSired  miN   maX   deFault     kP    kI    kD    duTy
LF Steer: 0       0        -90   90    0           1.70  0.10  3.00  0
RF Steer: 132     0        0     0     0           0.00  0.00  0.00  0
RR Steer: 127     0        0     0     0           0.00  0.00  0.00  0
LR Steer: 0       0        0     0     0           0.00  0.00  0.00  0
LF Drive: 0.0     0.0      0.0   0.0   0.0         0     0     0     ***
RF Drive: 0.0     0.0      0.0   0.0   0.0         0     0     0     ***
RR Drive: 0.0     0.0      0.0   0.0   0.0         0     0     0     ***
LR Drive: 0.0     0.0      0.0   0.0   0.0         0     0     0     ***
WaistPch: 25      0        0     0     0           0.00  0.00  0.00  0
WaistYaw: 45      0        0     0     0           0.00  0.00  0.00  0
L ArmPch: 53      0        0     0     0           0.00  0.00  0.00  0
L ArmYaw: 6   You are calibrating the LEFT FRONT STEERING joint.   0     0
L ArmRol: 1   Press j and l to move the joint to 0 DEGREES.        0     0
L ArmElb: 1  Current Analog Value: 121    Desired Analog Value:  121   0     0
L ArmWst: 153     0        0     0     0           0.00  0.00  0.00  0
R ArmPch: 153     0        0     0     0           0.00  0.00  0.00  0
R ArmYaw: 152     0        0     0     0           0.00  0.00  0.00  0
R ArmRol: 152     0        0     0     0           0.00  0.00  0.00  0
R ArmElb: 153     0        0     0     0           0.00  0.00  0.00  0
R ArmWst: 150     0        0     0     0           0.00  0.00  0.00  0
Head Pan: 0.0     0.0      0.0   0.0   0.0         0     0     0     ***
Head Tlt: 0.0     0.0      0.0   0.0   0.0         0     0     0     ***
L EyeCvg: 0.0     0.0      0.0   0.0   0.0         0     0     0     ***
R EyeCvg: 0.0     0.0      0.0   0.0   0.0         0     0     0     ***1
```

```
exit(ESC) actual  deSired  miN   maX   deFault     kP    kI    kD    duTy
LF Steer: 0       0        -90   90    0           1.70  0.10  3.00  0
RF Steer: 132     0        0     0     0           0.00  0.00  0.00  0
RR Steer: 127     0        0     0     0           0.00  0.00  0.00  0
LR Steer: 0       0        0     0     0           0.00  0.00  0.00  0
LF Drive: 0.0     0.0      0.0   0.0   0.0         0     0     0     ***
RF Drive: 0.0     0.0      0.0   0.0   0.0         0     0     0     ***
RR Drive: 0.0     0.0      0.0   0.0   0.0         0     0     0     ***
LR Drive: 0.0     0.0      0.0   0.0   0.0         0     0     0     ***
WaistPch: 25      0        0     0     0           0.00  0.00  0.00  0
WaistYaw: 45      0        0     0     0           0.00  0.00  0.00  0
L ArmPch: 53      0        0     0     0           0.00  0.00  0.00  0
L ArmYaw: 6  The calibration results are: (Press any key to exit.)  0     0
L ArmRol: 1            Slope A:  inf      Intercept A:  -inf       0     0
L ArmElb: 1            Slope B:  -90.000     Intercept B:  10890.000  0     0
L ArmWst: 153     0        0     0     0           0.00  0.00  0.00  0
R ArmPch: 153     0        0     0     0           0.00  0.00  0.00  0
R ArmYaw: 152     0        0     0     0           0.00  0.00  0.00  0
R ArmRol: 152     0        0     0     0           0.00  0.00  0.00  0
R ArmElb: 153     0        0     0     0           0.00  0.00  0.00  0
R ArmWst: 150     0        0     0     0           0.00  0.00  0.00  0
Head Pan: 0.0     0.0      0.0   0.0   0.0         0     0     0     ***
Head Tlt: 0.0     0.0      0.0   0.0   0.0         0     0     0     ***
L EyeCvg: 0.0     0.0      0.0   0.0   0.0         0     0     0     ***
R EyeCvg: 0.0     0.0      0.0   0.0   0.0         0     0     0     ***1
```

Figure 5-5: Calibration Utility

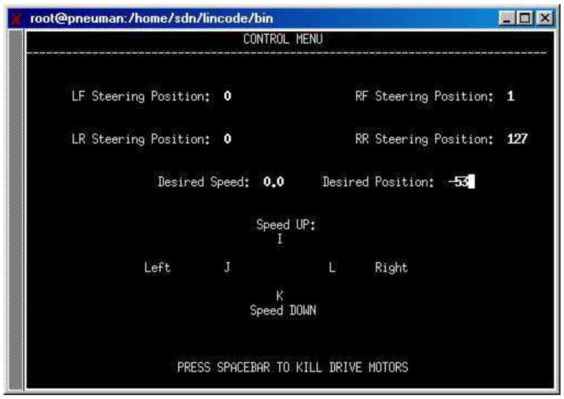

```
                              CONTROL MENU
--------------------------------------------------------------------------


   LF Steering Position:  0              RF Steering Position:  1


   LR Steering Position:  0              RR Steering Position:  127


              Desired Speed:  0.0      Desired Position:  -53


                             Speed UP:
                                 I

              Left       J              L       Right

                                 K
                             Speed DOWN



                   PRESS SPACEBAR TO KILL DRIVE MOTORS
```

Figure 5-6: Drive Control Menu

CHAPTER 6
DISCUSSION, FUTURE WORK, AND CONCLUSION

6.1 Discussion

Due to the popularization of humanoid robots in science fiction, many people may think that we are close to developing an artificial human. Robots from *The Terminator* and *Artificial Intelligence* appear to function in our society. They blend in and possess abilities equal, if not superior, to their human creators. However, both films confront problems that can arise from humanoid robots. These problems are not new; the first use of the word *robot* mentions them overtaking their human creators. Should we worry? No. Today's most advanced robotic systems cannot “think” for themselves. They have trouble walking up stairs and identifying and grasping objects. All of these tasks, trivial to humans, are prohibitively complex for humanoids.

Upon researching the state-of-the-art humanoids, it is clear that we are at the very beginning of our science fiction fantasies. The most mechanically advanced self-contained humanoid, the Honda *P3*, is primarily programmed [11]. Scenes on television of this robot walking down stairs and opening doors may have led some to believe that we are close the realization of science fiction. However, laymen do not know that millions of dollars have been spent to achieve this goal. They do not know that there were hundreds of engineers and scientists who programmed every move the robot made. They do not know that the robot did not think about walking down the stair or opening the door. It was explicitly told to move each foot, bend each knee, and rotate the elbow joint. The robot has no idea of what stairs or doors *are*.

The quest to build a humanoid robot must be considered carefully. Because humans are so complicated, a divide-and-conquer approach is used. Many researchers are developing systems that accomplish specific tasks needed for a humanoid, such as computer vision, voice recognition, and speech synthesis. Even if all of the individual humanoid systems were perfected, how should they be integrated? Will the combination of these systems be enough to make a robot think? A famous quote from Newell and Simon appears to summarize the problem of "thinking":

> I want to take my son to nursery school. What's the difference between what I have and what I want? One of distance. What changes distance? My automobile. My automobile won't work. What is needed to make it work? A new battery. Who has new batteries? An auto repair shop. I want the shop to put in a new battery; but the shop doesn't know I need one. What is the difficulty? One of communication. What allows communication? A telephone . . . and so on. [30:15]

6.2 Future Work

6.2.1 Overall Implementation

The research and development of *Pneuman* and the humanoid systems will be an ongoing project at the MIL. Before significant humanoid specific research can be accomplished, all of the underlying control and sensor systems must be implemented. This includes the control systems for the dual five DOF arms, the waist assembly, the neck assembly, and the active stereo head. The sensor systems may include the machine vision system, obstacle avoidance systems, voice recognition systems, and navigation systems.

Unfortunately, due to time constraints, all of the control systems needed to control *Pneuman's* joints have not been implemented. The neck, arms, and head are still under construction. After these assemblies are completed and mechanically integrated on to *Pneuman*, the control systems must be updated and revised to implement the PID control methods and trajectory generation discussed in the previous sections. This also includes the implementation of the forward and inverse kinematics and dynamic modelling of the robot.

6.2.2 Future Research

As discussed earlier, there is a wide spectrum of systems that need to be developed for the realization of a practical humanoid robot. All of the systems can not be discussed, however, some of the possibilities of future research that may be applied to *Pneuman* deal with control improvement techniques, voice recognition, computer vision, and navigation.

The objectives of *Pneuman's* control systems are to move the joints in the manner specified by the trajectory generation module. This is accomplished adequately by using a PID control law, but there are still errors between the desired and actual trajectories. These errors may be attributed to inaccuracies with the feedback sensors, the dynamic models, friction, or a number of other non-modelled factors. Machine learning techniques may be used to reduce the error between the desired and actual trajectories. A proposed scheme is illustrated in Figure 6-1. This scheme augments the current control system with a *trainable* module. Data may be collected during execution of trajectories and used to train the module. The module will "learn" the errors in the untrained system and compensate for them, thereby reducing the error in the augmented system [31].

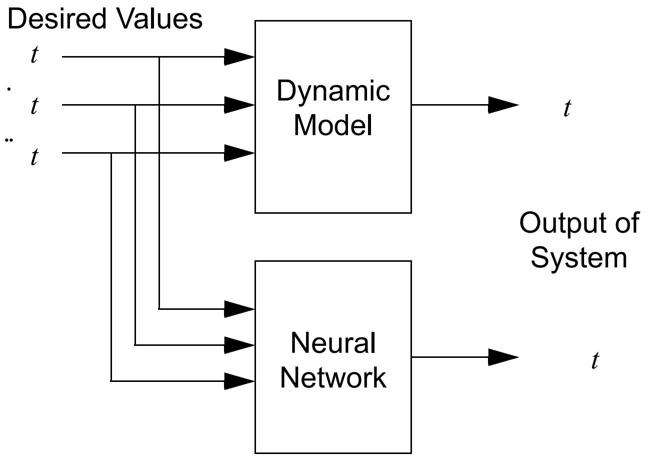

Figure 6-1: Augmented control scheme

Voice recognition is an important aspect of humanoid development. This natural communication technique is the preferred method of interaction with humanoids. With recent advances in voice recognition hardware and software, a feasible system can be implemented for *Pneuman* with minimal effort. These commercial off the shelf systems may be improved upon with the addition of a natural language processing (NLP) system. A NLP system would give *Pneuman* the ability to process and understand complex phrases.

Pneuman's active stereo head will be an ideal platform for stereo vision research. Implementation of the control and vision system will give *Pneuman* the ability to use machine learning techniques to identify the location of objects in 3D space. The cameras will use wireless video transmitters, permitting off-board image analysis. This means that the vision processing is not limited to the on-board computing power and the limitations of an embedded computer system will not hinder the vision research.

Navigation and path planning should also be addressed. The optical encoders mounted on *Pneuman* wheels provide accurate wheel position information which can be used for dead reckonining. This technique can be coupled with a local positioning system, allowing *Pneuman* to navigate in a building or similar environment. A global positioning system (GPS) can be used outdoors for long range navigation. These features can help *Pneuman* operate autonomously in any environment.

6.3 Conclusion

In spite of the difficulties, research must start somewhere. That is why *Omnibot* was created. It was a first attempt to integrate a few humanoid systems at a low cost. The robot was able to move around without bumping into objects. It was able to talk to an audience and give presentations. It could understand a few simple phrases, and it could communicate verbally. All of these behaviors were programmed, just as with the Honda *P3* robot, but *Omnibot* cost approximately $500.00.

Omnibot was not designed to withstand the rigors of everyday use. Repeated presentations and self-demonstrations took a toll on the robot, causing major mechanical failures. Fortunately, the idea of a humanoid robot giving tours of the Machine Intelligence Laboratory was well received. The idea that a *robot* could tell you about other robotic projects in the lab is interesting and entertaining. Therefore *Pneuman* will satisfy the need for entertainment and serve as a more reliable humanoid robot research platform. *Pneuman* is still under construction, but when it is finished, its abilities will exceed that of *Omnibot*. *Pneuman* will have more computing power, more degrees of freedom, more sensors, and it will be a more reliable research platform.

Upon examining the creations from our ancestors, we can see that people have always desired to recreate their own form. It wasn't always for religious purposes; as humans *we* want to know how *we* work, how *we* think, and how *we* feel. It wasn't until recent years that technology has advanced far enough to develop humanoids, therefore the development of humanoid robots is relatively new. Humanoid development is in its infancy and the current state of the art may not appear to be significant. Fortunately, researchers will continue to improve technology and search for ways to achieve the "holy grail" of roboticists: to develop an autonomous humanoid robot.

APPENDIX A
MECHANICAL DRAWINGS

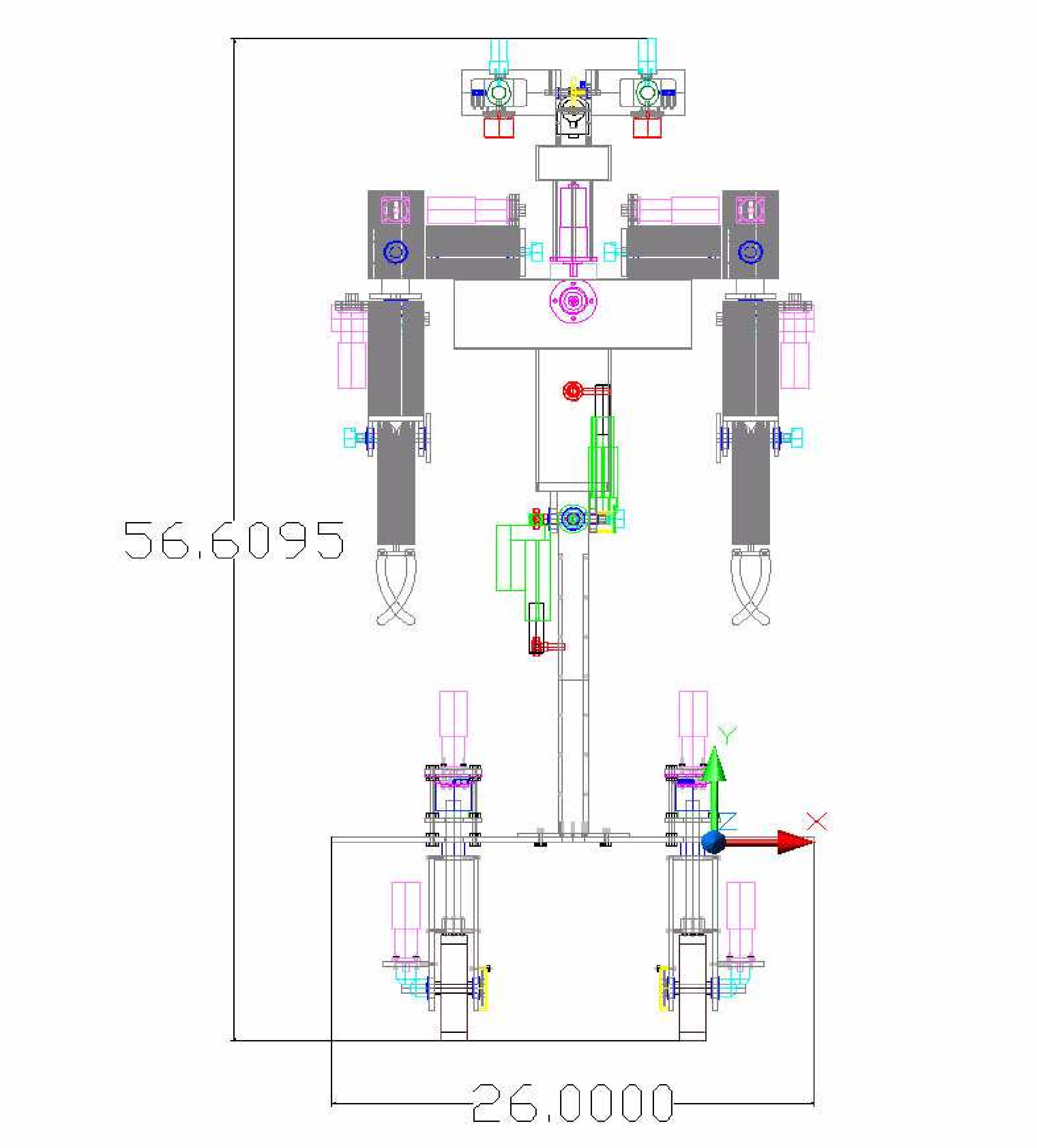
56.6095
Y
Z
X
26.0000

Figure A-1: Front view of *Pneuman*

APPENDIX B
SCHEMATICS

B.1 Pulse Width Modulation (PWM) pc/104 Card

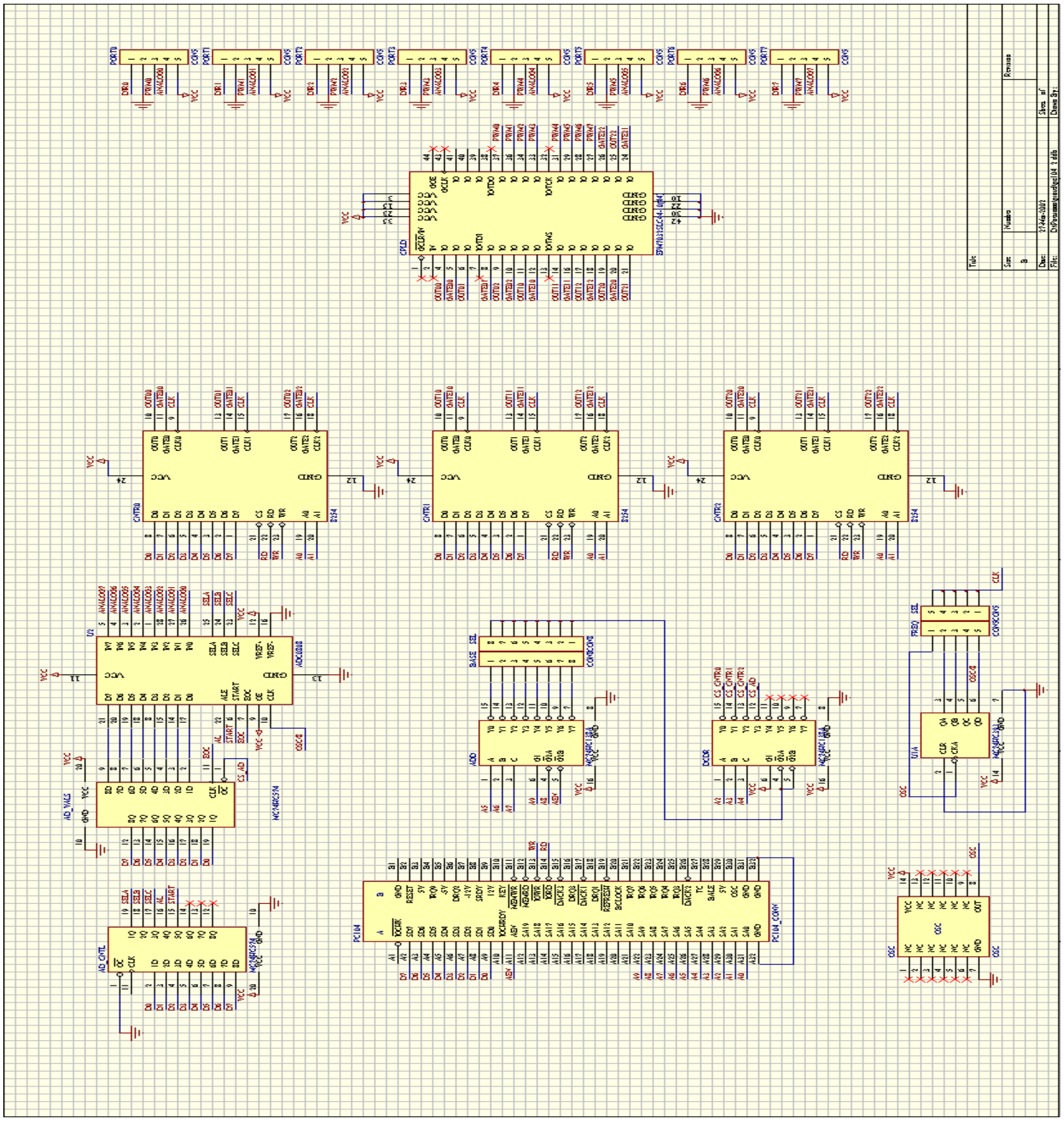

PORT0
PORT1
PORT2
PORT3
PORT4
PORT5
PORT6
PORT7
CON5
DIR0
PWM0
ANALOG0
VCC
CPLD
EPM7032SLC44-10
CNTR0
CNTR1
CNTR2
8254
OUT0
GATE0
CLK0
GND
ADC0808
AD_VALS
AD_CNTL
MC74HC574
ADD
DCDR
MC74HC138A
BASE
SEL
FREQ
OSC
PC104
PC104_CONN
Title
Size
Number
Revision
Date:
File:
Sheet of
Drawn By:

Figure B-1: PWM pc/104 card schematic

B.2 LM629 pc/104 Card

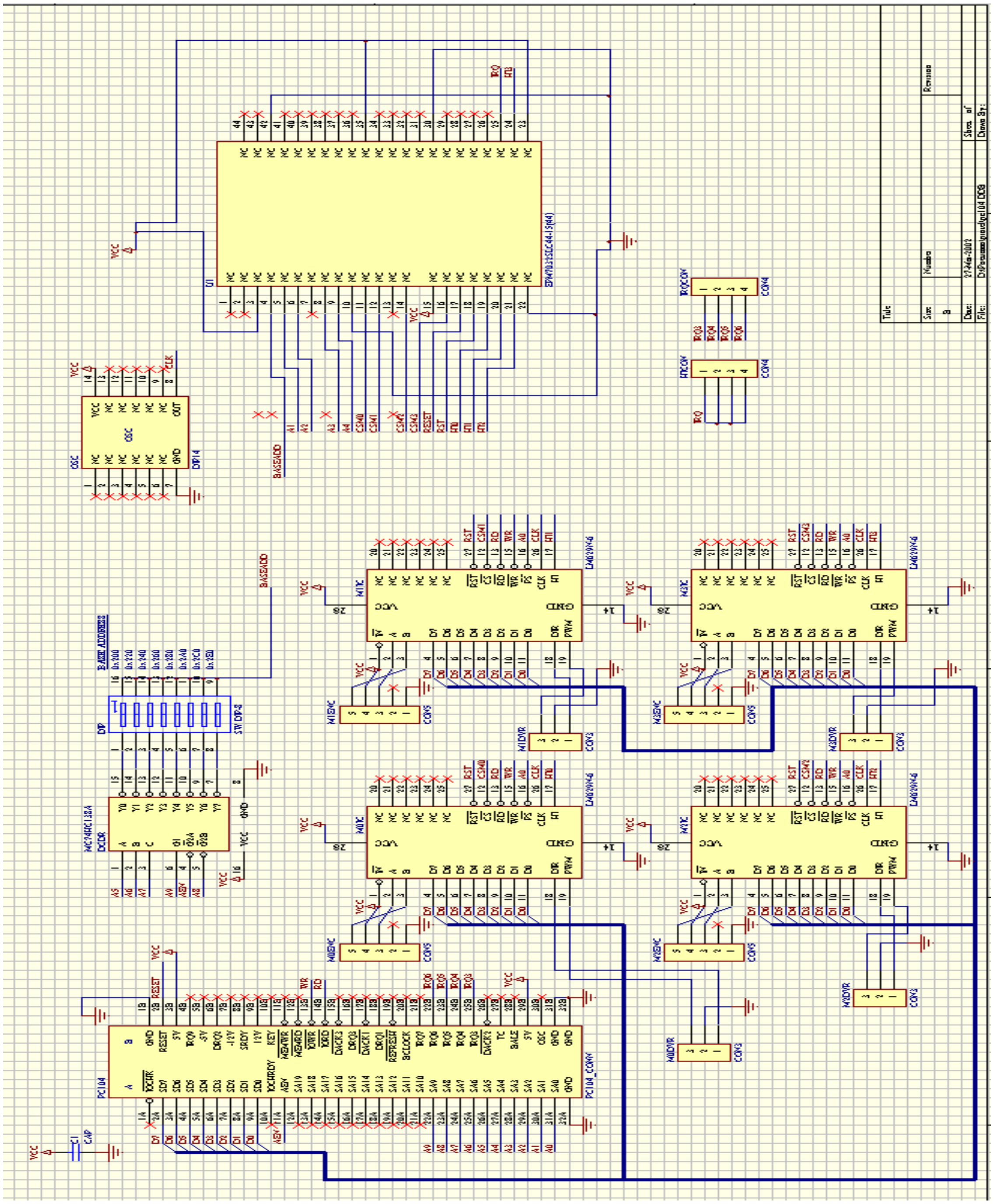

EPM7032SLC44-5(44)
U1
OSC
DIP14
BASE ADDRESS
SW DIP-8
DIP
MC74HC138A
DCDR
LM629N-6
PC104
PC104_CONN
CAP
C1
VCC
BASEADD
Title
Size
Number
Revision
Date:
File:
Sheet of
Drawn By:

Figure B-2: LM629 pc/104 card schematic

REFERENCES

[1] Menzel, P.; D'Aluisio, F., *Robosapiens: Evolution of a New Species*, The MIT Press, Cambridge, Massachusetts, 2000, Pages 16 and 18.

[2] Brinton, C.; Christopher, D.; Wolf, A., *A History of Civilization, Volume 1: Prehistory to 1715*, Prentice-Hall, Inc., Englewood Cliffs, New Jersey, 1955, Pages 8, 9, 27, and 29.

[3] Kinnaer, J., *The Ancient Egypt Site: From A to Z,* 2/15/1997, http://www.geocities.com/~amenhotep/glossary/index.html, accessed 1/05/2002.

[4] Botsford M.; Robinson P., *Hellenic History,* Fourth Edition, The Macmillan Company, New York, New York, 1956, Plates 1, 5, 32, and 100.

[5] Drachman, A., *Ktesibios, Philon and Heron: A Study in Ancient Pneumatics*, Copenhagen: Munksgaard,1948.

[6] Rosheim, Mark E., *Robot Evolution: The Development of Anthrobotics*, John Wiley & Sons, Inc., New York, New York, 1994.

[7] Dowling, K., *What is Robotics?,* 1996, http://www.frc.ri.cmu.edu/robotics-faq/1.html, accessed 1/10/2002.

[8] Fukuda, T.; Michelini, R.; Potkonjak, V.; Tzafestas, S.; Valavanis, K.; Vukobratovic, M., "How Far Away is Artificial Man?" IEEE Robotics & Automation Magazine, Volume 8 Issue 1, March 2001, Pages 66-73.

[9] Koku A.; Sekmen A.; Alford A., "Towards Socially Acceptable Robots," 2000 International Conference on Systems, Man, and Cybernetics, Volume 2, Pages 894-899, 2000.

[10] Swinson, M.L.; Bruemmer, D.J., "Expanding Frontiers of Humanoid Robotics," IEEE Intelligent Systems, July-Aug. 2000, Volume 15, Issue 4, Pages: 12-17

[11] Hirai, K.; Hirose, M.; Haikawa, Y.; Takenaka, T., "The Development of Honda Humanoid Robot," Proceedings of the 1998 IEEE International Conference on Robotics and Automation, 1998, Volume 2, Pages: 1321-1326.

[12] Konno, A.; Kato, N.; Shirata, S.; Furuta, T.; Uchiyama, M., "Development of a Lightweight Humanoid Robot," Proceedings of the 2000 IEEE/RSJ International Conference on Intelligent Robots and Systems (IROS 2000), Volume 3, Pages 1565-1570.

[13] Price, A.; Jarvis, R.; Russell, R.A.; Kleeman, L., "A Lightweight Plastic Humanoid Robot," Proceedings of the 2000 IEEE/RSJ International Conference on Intelligent Robots and Systems, (IROS 2000), Volume 3, Pages 1571-1576.

[14] Lim, H. O.; Takanishi, A., "Waseda Biped Robots Realizing Human-like Motion," Proceedings of the 6th International Workshop on Advanced Motion Control, 2000, Pages 525-530.

[15] Ambrose, R.O.; Aldridge, H.; Askew, R.S.; Burridge, R.R.; Bluethmann, W.; Diftler, M.; Lovchik, C.; Magruder, D.; Rehnmark, F., "Robonaut: NASA's Space Humanoid," IEEE Intelligent Systems, July-August 2000, Volume 15, Issue 4, Pages 57-63.

[16] Nagakubo, A.; Kuniyoshi, Y.; Cheng, G., "Development of a High-Performance Upper Body Humanoid System," Proceedings of the 2000 IEEE/RSJ International Conference on Intelligent Robots and Systems (IROS 2000), Volume 3, Pages 1577-1583.

[17] Morita, T.; Iwata, H.; Sugano, S., "Development of Human Symbiotic Robot: WENDY," Proceedings of the 1999 IEEE International Conference on Robotics and Automation, Volume 4, Pages 3183-3188.

[18] Lee S.; Park S.; Kim M; Lee C., "Design of a Force Reflecting Master Arm and Master Hand using Pneumatic Actuators," Proceedings of the 1998 IEEE International Conference on Robotics and Automation, Volume 3, Pages 2574-2579.

[19] Caldwell, D.G.; Tsagarakis, N.; Artrit, P.; Canderle, J.; Davis, S.; Medrano-Cerda, G.A., "Biomimetic and Smart Technology Principals of Humanoid Design," Proceedings of the 2001 IEEE/ASME International Conference on Advanced Intelligent Mechatronics, Volume 2, Pages 965-970.

[20] Taddeucci, D.; Dario, P.; Ansari, E., "An Approach to Anthropomorphic Robotics: Guidelines and Experiments," Proceedings of the 1999 IEEE/RSJ International Conference on Intelligent Robots and Systems, (IROS 1999), Volume 1, Pages 537-542.

[21] Tevatia, G.; Schaal, S., "Inverse Kinematics for Humanoid Robots," Proceedings of the 2000 IEEE International Conference on Robotics and Automation, Volume 1, Pages 294-299.

[22] Yamato, J., "A Layered Control System for Stereo Vision Head with Vergence," Conference Proceedings of the 1999 IEEE International Conference on Systems, Man, and Cybernetics (IEEE SMC 1999), Volume 2, Pages 836-841.

[23] Adams, B.; Breazeal, C.; Brooks, R.A.; Scassellati, B., "Humanoid Robots: A New Kind of Tool," IEEE Intelligent Systems, July-Aug. 2000, Volume 15, Issue 4, Pages 25-31.

[24] Nortman, S.; Arroyo, A.; Schwartz, E., "Omnibot 2000: Development of an Autonomous Mobile Agent for the Disabled and Elderly," Proceedings of the 2000 Florida Conference on Recent Advances in Robotics, Volume 6, Pages 51-58.

[25] *Webster's Universal College Dictionary*, Random House, Inc., New York, New York, 1997.

[26] Jones J.; Flynn A., *Mobile Robots Inspiration to Implementation,* A K Peters, Ltd., Natick, Massachusetts, 1993.

[27] Nortman, S.; Peach, J.; Nechyba, M.; Brown, L.; Arroyo, A., “Construction and Kinematic Analysis of an Anthropomorphic Mobile Robot”, Proceedings of the 2001 Florida Conference on Recent Advances in Robotics, Volume 7, Pages 32-42.

[28] National Semiconductor Corporation, “LM628/LM629 Precision Motion Controller”, product datasheet, 11/01/1999, http://www.national.com/ds/LM/LM629.pdf, accessed 9/20/2000.

[29] Craig, J., *Introduction to Robotics: Mechanics and Control,* 2nd Edition, Addison-Wesley Publishing Company Inc., Reading, Massachusetts,1989.

[30] Newell A.; Simon, H., “GPS: A Program that Simulates Human Thought”, *Computers and Thought*, ed. Feigenbaum and Feldman, McGraw-Hill, Cambridge, Massachusetts, 1963, Pages 34-48.

[31] Nechyba, M., EEL 6935 Machine Learning II, “Neural Networks and Their Applications,” Class Notes, Fall 2001.

BIOGRAPHICAL SKETCH

Scott Nortman was born and raised in Hollywood, Florida. He graduated from the University of Florida in August, 2000 with a Bachelor of Science degree in electrical engineering. Scott continued his studies and received his Master of Science degree in May, 2002. His area of specialization was intelligent systems. Scott moved to Palo Alto, California in July, 2002 to work for Lockheed Martin. He is considering pursuing his Ph. D. after gaining experience in the industry.